Construction of a 1° × 1° fossil fuel emission data set for carbonaceous aerosol and implementation and radiative impact in the ECHAM4 model

W.F. Cooke,[1] C. Liousse, and H. Cachier

Laboratoire des Sciences du Climat et de l'Environnement, Laboratoire Mixte CNRS-CEA, Gif sur Yvette, France

J. Feichter

Max Planck Institut für Meteorologie, Hamburg, Germany

Abstract. Global-scale emissions of carbonaceous aerosol from fossil fuel usage have been calculated with a resolution of 1° × 1°. Emission factors for black and organic carbon have been gathered from the literature and applied to domestic, transport, and industrial combustion of various fuel types. In addition, allowance has been made for the level of development when calculating emissions from a country. Emissions have been calculated for 185 countries for the domestic, industrial, and transport sectors using a fuel usage database published by the *United Nations* [1993]. Some inconsistencies were found for a small number of countries with regard to the distribution of fuel usage between the industrial and domestic sectors. Care has been taken to correct for this using data from the fuel use database for the period 1970-1990. Emissions based on total particulate matter (TPM) and submicron emission factors have been calculated. Global emissions for 1984 of black carbon total 6.4 TgC yr^{-1} and organic carbon emissions of 10.1 TgC yr^{-1} were found using bulk aerosol emission factors, while global black carbon emissions of 5.1 TgC yr^{-1} and organic carbon emissions of 7.0 TgC yr^{-1} were found using submicron emission factors. Use of the database is quite flexible and can be easily updated as emission factor data are updated. There is at least a factor of 2 uncertainty in the derived emissions due to the lack of exactly appropriate emission data. The emission fields have been introduced into the ECHAM4 atmospheric general circulation model and run for 5 model years. Monthly mean model results are compared to measurements in regions influenced by anthropogenic fossil fuel emissions. The resultant aerosol fields have been used to calculate the instantaneous solar radiative forcing at the top of the troposphere due to an external mixture of fossil fuel derived black carbon and organic carbon aerosol. Column burdens of 0.143 mgBC m^{-2} and 0.170 mgOC m^{-2} were calculated. Because of secondary production of organic carbon aerosol, it is recommended that the burden of organic carbon aerosol be doubled to 0.341 mgOC m^{-2}. The resultant forcing when clouds are included is +0.173 W m^{-2} for black carbon and -0.024 W m^{-2} for organic carbon (×2) as a global annual average. The results are compared to previous works, and the differences are discussed.

1. Introduction

There is concern about the changing composition of the atmosphere due to anthropogenic emissions. It is predicted that emissions of so-called greenhouse gases could cause a warming of the atmosphere by several degrees on a regional scale. To date, studies of the radiative impact of anthropogenic aerosols include the effect of sulphate [*Charlson et al.*, 1991, 1992; *Kiehl and Briegleb*, 1993; *Taylor and Penner*, 1994; *Feichter et al.*, 1997] , an external mixture of sulphate and black carbon [*Haywood and Shine*, 1995; *Schult et al.*, 1997] , biomass-burning particles [*Penner et al.*, 1992; *Hobbs et al.*, 1997], and anthropogenic dust aerosol [*Tegen and Lacis*, 1996; *Tegen et al.*, 1996]. These studies have found that mixtures of various aerosols tend to have a cooling effect on the atmosphere, but not all the aerosol types found in the atmosphere have been included.

A consequence of the combustion of fossil fuel is the emission of carbonaceous aerosol. Different combustion processes emit different amounts of carbonaceous aerosol as a consequence of the efficiency of the combustion process. This carbonaceous aerosol can be broken into two fractions, an organic carbon (OC) fraction which may be reactive in the atmosphere and a nonreactive black carbon (BC) fraction. The optical properties of these two fractions are also quite dissimilar. The organic fraction has optical properties which are mainly scattering in the solar spectrum. The BC aerosol is, as its name suggests, highly absorbing in the solar spectrum and is the only ubiquitous aerosol with a significant absorption cross section. The abundance of OC as a fraction of the carbonaceous aerosol may differ significantly because of the combustion process and fuel type. In less efficient processes the OC fraction of the carbonaceous aerosol is more significant. The ratio BC:OC may not be constant in the atmosphere because of differing lifetimes and sources, and *Penner et al.* [1995] with a simple box model has shown that the radiative forcing of the atmosphere is quite sensitive to the ratio of BC to OC emission.

While the majority of modeling efforts have concentrated on the sulphur cycle, it is also necessary to calculate the global mass distribution of carbonaceous aerosol in order to provide a better picture of the impact of anthropogenic emissions on the atmosphere and the impacts on radiative transfer thereof. Recent studies and experiments have found that the OC mass concentration in both anthropogenically influenced source and remote areas may be of the same magnitude as that of sulphate [*Cachier et al.*, 1990; *Novakov and Corrigan*, 1996; *Hegg et al.*, 1997].

The main purpose of this work is to improve the fossil fuel carbonaceous aerosol inventory and to show where some of the uncertainties may lie. This work presents an exhaustive inventory of primary carbonaceous aerosol from fossil fuel combustion. Previous inventories from *Penner et al.*, 1993] and *Cooke and Wilson* [1996] all concentrated on the emission of BC from either or both of fossil fuel and biomass burning. *Liousse et al.* [1996] was the first to include organic aerosol on a global scale with a detailed work on biomass-burning emissions while scaling the fossil fuel emissions from the emissions of BC of *Penner et al.* [1993]. The work presented here improves on the works of *Cooke and Wilson* [1996] and *Liousse et al.* [1996] by compiling consistent updated data sets of both BC and OC emissions from the combustion of fossil fuels and their various usages. This work also corrects some errors made in previous fossil fuel carbonaceous aerosol inventories where BC emission factors were implicitly equated to total particulate matter emission factors. In addition, we utilize the level of development of a country to differentiate between the efficiency and control of emissions in various countries. Furthermore, the previous studies of carbonaceous aerosol emission have been mainly based on bulk emission factors. The dry deposition velocity of particles with diameters of greater than a few microns is such that the lifetime of these particles is quite short. Therefore, when using global models with grid boxes of several square degrees, it is necessary to concentrate on the fraction of the aerosol which is capable of long-range transport.

In this work we calculate emission factors on the basis of submicron emissions. The submicron and bulk emissions may give us an idea of the lower and upper limits of the impacts of global emission of primary carbonaceous aerosol from the combustion of fossil fuel. In this work we also calculate the mass distribution of carbonaceous aerosol emitted from fossil fuel sources using the fourth generation Max-Planck-Institute model, ECHAM4, which is the most recent in a series evolving from the European Centre for Medium-Range Weather Forecasts (ECMWF) model. In this study the T30 version of the model is used, which has an approximate resolution of $3.75° \times 3.75°$. Although this is not the finest resolution of the model, the T30 resolution was chosen because of computational time constraints. It should be noted here that the resolution of the model will cause some problems when comparing the results with mea-

[1]Now at Geophysical Fluid Dynamics Laboratory, Princeton, New Jersey

surements made near source regions. Improved optical properties of carbonaceous particles are implemented in the radiative code of the ECHAM4 model in order to obtain preliminary results of the radiative forcing of carbonaceous aerosol emitted by fossil fuel based combustion.

2. Method

The quantity of carbonaceous aerosol emitted by fossil fuel combustion is proportional to the quantity of fuel consumed and the emission factor for the combustion process. The quantity of fuel consumed is reasonably well known, and we use a fossil fuel consumption data set from the *United Nations* [1993] to calculate these quantities. The year 1984 was chosen as the reference year for this study. The seasonality of the combustion of fossil fuel has been taken from *Rotty* [1987]. The emission factor for the combustion of a particular fuel is a complicated function of various parameters, such as temperature and oxygen availability. There is a paucity of emission factor data for carbonaceous aerosol and, especially, OC. There is, however, much more data available for total particulate matter (TPM) over a range of industrial and domestic situations. We will use a combination of TPM and BC emission factors in order to extrapolate BC emission factors for various consumption sectors. Emission factors for OC have been reported only for developed countries. Therefore, in order to compile a consistent data set of BC and OC emission factors, we have used the ratio of OC to BC for each fuel type to scale the emission factor of OC for the same consumption sector for other countries. The method used here accounts only for primary production of OC. Secondary production of OC aerosol contributes a large fraction of the OC aerosol mass. The secondary production is not calculated explicitly in this model at this time but account is taken (section 6.2) of this aerosol when calculating the radiative forcing of carbonaceous aerosol.

2.1. Differentiation of Emission Factors by Country

The method used in this paper is based on that used in the calculation of fossil fuel emissions of BC by *Cooke and Wilson* [1996], and the distribution scheme is shown in Figure 1. There is an improvement in the distribution of emissions in that in the work presented here, a differentiation has been made with respect to the level of development of the 185 countries in the database. The level of development of a country has

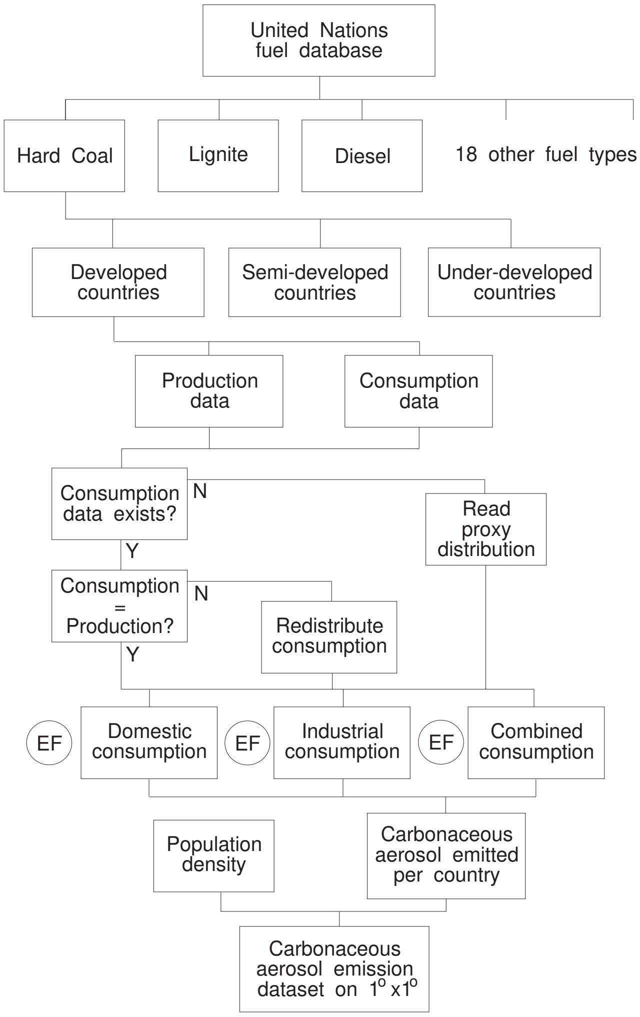

Figure 1. Tree diagram of emission distribution.

consequences for the emission of carbonaceous aerosol as combustion tends to be more efficient. Furthermore, governments of developed countries legislate to reduce emissions from industrial and vehicular sources. In less developed countries, control of emissions are not such a high priority, and emission sources are replaced by more efficient modern equipment at a slower rate than in developed countries. Similarly, vehicles tend to be older and are not as expertly maintained in less developed countries. These older cars will be the source of much greater emissions than in the developed countries. Therefore one can expect that there will be a variation in the emission factor of carbonaceous aerosol between the same combustion process in different countries, and it is necessary to make some differentiation between countries on the basis of their level of development and not simply use distribution maps of the consumption of fuels to calculate emissions. We have placed the countries of the world into three groupings, representing developed, semideveloped, and developing countries. The group of developed countries is composed of the members of the Organization for Economic Cooperative Development (OECD) in 1984. The semideveloped countries are considered to be the countries of the former Eastern European bloc, the former USSR, South Africa, Israel, Hong Kong, Singapore, and Taiwan. All other countries were placed in the group of developing countries.

2.2. Differentiation of Emission Factors by Combustion Process

There are various differences between the emission characteristics of domestic and industrial processes. The relatively poorer conditions of domestic combustion, compared to industrial combustion, will favor the production of particles. In addition to the difference between domestic and industrial processes, there are also differences within the industrial sector with respect to the efficiency of the equipment used in various processes. Data from the United States *Environmental Protection Agency (EPA)* [1994] show that emission factors for particulate matter of less than 10 μm (PM-10) from coal-burning electric utilities in the United States decreased by a factor of 15 between 1970 and 1990. This shows that there has been an improvement in the efficiency of combustion and control of emissions in the developed world over time. In China the utilization efficiency of energy is approximately 30% less than in the developed world [*Zhang et al.*, 1994]. The lower efficiency of this equipment may result in lower temperatures and therefore relatively higher emission factors.

In addition, the relative fractions of BC and OC in the carbonaceous aerosol are different for the domestic and industrial settings. We may assume that the organic fraction of the aerosol is not as important in industrial settings as in domestic settings because of the higher temperatures for industrial combustion. This is also corroborated from our experience of the changes in BC to OC ratios with temperature in vegetation fires [*Cachier et al.*, 1995]. The relatively lower temperature of domestic combustion will result in less thermal degradation of the fuel and therefore will lead to a greater fraction of organic aerosol. In industrial processes the temperature of combustion allows the fuel to thermally degrade to a greater extent, and the organic fraction of the emissions will also combust, meaning that the BC emissions are relatively more important in this case.

The fuel use data set which we used to calculate the amount of fuel used in domestic or industrial settings also includes some categories of usage that are not clearly one or the other. In this case we have used a so-called "combined" emission factor to estimate the emissions from these sources. This emission factor is simply the square root of the product of the domestic and industrial emission factors. An exception to this is made for diesel and motor gasoline, where the combined sector is replaced by a traffic sector for which an emission factor is specifically calculated.

In résumé, we have divided the countries into three levels of development. For each of these levels of development, there is also a division made between domestic, industrial, and traffic or combined usage of each fuel type. Therefore, for each fuel type it is necessary to calculate nine emission factors.

2.3. Consideration of Size Distribution in Calculating Emission Factors

A problem with using bulk emission factors is that carbonaceous aerosol may consist of particles with particle radii ranging over several orders of magnitude. For instance, the largest particles emitted from coal burning, fly-ash, may be several hundreds of microns in diameter [*McElroy et al.*, 1982]. However, particles of this size range will have very large deposition velocities and will not remain in the atmosphere for very long. The particles with the lowest deposition velocities, and therefore longest lifetime with respect to dry deposition, are submicron aerosol particles. It is therefore useful to evaluate the submicron fraction of carbonaceous aerosol emissions as we are interested in implementing these emissions in a global transport model where the aerosol size distribution is considered constant. The submicron aerosol is also the size range of aerosol particles where the radiative effects of aerosol are at a maximum. It should be noted that because of the paucity of data, no consideration has been made of the carbon content of the bulk emissions as a function of size in this work.

In considering bulk and submicron emission factors, the majority of data on size distributions of emissions exist for coal and diesel only. These fuels are the source of the majority of the carbonaceous emissions, while other sources, although important locally, contribute relatively little to the global emissions. As BC and OC are coemitted from fossil fuels when burnt, we will assume that the size distributions of the two species are similar [*Brémond et al.*, 1989].

For coal combustion, bulk emission factors are generally derived from uncontrolled emission factors. However, in industrialized countries, there are also control devices fitted to further reduce the emissions. These control devices generally have a high total mass removal efficiency with legislation requiring that up to 99% of the mass be removed. Control devices generally use the aerodynamic properties of aerosol to assist in their removal. However, the removal efficiency of these devices deteriorates as the size of the particle decreases. Therefore, while a device may claim a removal efficiency of 99% of the mass, this will be true only for the entire size range of the particles, not for submicron particles. The *EPA* [1996] reports the uncontrolled and controlled emission factors of submicron PM for various control devices in conjunction with various combustion devices. The control devices are given in Table 1 along with the appropriate submicron emission factor, where it can be seen that the control device can remove between 10 and 99% of the mass of the submicron aerosol. We will assume an average (50%) over all the devices in calculating the reduction in submicron emission factors for developed countries because of control of emissions.

Coal has a large mass fraction in the supermicron fraction of its emissions [*Schure et al.*, 1985; *McElroy et al.*, 1982]. For the industrial use of coal we used data from the *EPA* [1996] for the submicron fraction of uncontrolled TPM emissions from various combustion devices (Table 2) and data from *McElroy et al.* [1982] on the ash content of hard coal. Assuming that each of BC and OC comprise 25% of the submicron aerosol, we obtain a submicron emission factor for industrial coal usage. It should be noted that this assumption introduces some uncertainty into the data set as the fraction of submicron PM which is carbonaceous probably varies with the combustion conditions. For domestic situations the *EPA* [1996] report that submicron PM constitute 50% of bulk emissions. This will apply to submicron BC and OC emission factors as well.

Several authors have reported concordant results on size distributions of diesel emissions using impactors and/or electron microscopy. These studies show that the mass distribution peaks in the accumulation mode [*Whitby*, 1978; *Horvath et al.*, 1988; *Weingartner et al.*, 1997]. We will assume that all carbonaceous particulate matter emitted by diesel engines are submicron.

2.4. Major Sources of Carbonaceous Aerosol

The emission factors for each fuel type and each industrialization sector are given in Table 3a for BC and Table 4 for OC. A summary of the emission factors found in the literature and used in calculating the average BC emission factor for several fuels in developed countries are given in Table 3b.

The "standard" procedure we use to calculate the nine emission factors for each fuel type is as follows. Emission factors are generally representative of developed countries. The average emission factor in Table 3b was selected for domestic or industrial usage of fossil fuels in developed countries. For domestic usage the maximum in the range of the emission factors was used as the average emission factor for semideveloped and underdeveloped countries. For industrial usage in underdeveloped countries we assume that the emission factor is 5 times that of developed countries [*Etemad and Luciani*, 1991], whereas for semideveloped countries the average emission factor was assumed to be the maximum of the range of those found for "developed" countries. The factor of 5 used here is probably on the conservative side. In all cases the combined sector emission factor is calculated as the square root of the product of the domestic and industrial emission factors. Exceptions to this procedure will be pointed out in the following where necessary. The same procedure is used for both BC and OC.

2.4.1. Coal. The BC emission factors for hard coal have been derived in the standard manner. For OC, there are very few measurements of the emission from hard coal combustion. Most of these refer to measurements of extractable organic matter which may represent only about 60% of the total organic matter [*Rogge et al.*, 1993]. Therefore one needs to divide this emission factor by 0.6 in order to correct for the nonextractable organic matter. In order to calculate the emission of organic carbon, one also needs to divide the organic matter emission rate by a factor of 1.4 [*Duce*, 1978; *Countess et al.*, 1981]. The domestic emission factors

Table 1. Uncontrolled and Controlled Submicron Emission Factors

Type of Control Device	Uncontrolled Emission Factor	Controlled Emission Factor	Ratio Control/Uncontrolled
Multiple cyclone	0.2A*	0.02A	0.1
no reinjection of	3.3	0.4	0.12
fly-ash	0.28A	0.26A	0.93
	2.0	3.6	1.8
Multiple cyclone reinjection of fly-ash	3.3	1.6	0.48
Scrubber	0.2A	0.18A	0.9
Electrostatic	0.2A	0.01A	0.05
precipitator	0.28A	0.004A	0.014
	3.3	0.2	0.06
Bag-house	0.2A	0.006A	0.03
	3.3	0.018	0.0055
Average	...	...	0.408

Emission factors are from the *EPA* [1996]

*A is the weight percent ash content of coal. If the ash content is 12.8%, then A=12.8.

Table 2. Uncontrolled Bulk and Submicron Emission Factors

Coal Combustion Device	Bulk Emission Factor, g kg^{-1}	Submicron Emission Factor, g kg^{-1}
Pulverised coal dry bottom	5A*	0.1A
Pulverised coal wet bottom	3.5A	0.14A
Spreader stoker	33	1.65
Overfeed stoker	8	0.96
Underfeed stoker	7.5	1.575

Emission factors are from the *EPA* [1996]

*A is the weight percent ash content of coal. If the ash content is 12.8%, then A=12.8, leading to emission factors of 64 gTPM kg^{-1} and 44.8 gTPM kg^{-1} for the two types of pulverised coal burner.

Table 3a. Emission Factors for Bulk Black Carbon Aerosol

Fuel Type	Sector	Underdeveloped, g kg^{-1}	Semideveloped, g kg^{-1}	Developed, g kg^{-1}
		Bulk BC Emission Factors		
Hard coal, hard coal briquettes, coke oven coke, gas coke, brown coal coke	combined	2.13	1.22	0.75
	domestic	4.55	4.55	2.78
	industrial	1.0	0.325	0.2
Lignite brown coal, lignite briquettes	combined	3.84	2.2	1.34
	domestic	8.18	8.18	5.0
	industrial	1.8	0.59	0.36
Diesel	transport	10.0	10.0	2.0
	domestic	2.0	2.0	2.0
	industrial	0.35	0.09	0.07
Peat	combined	0.3	0.3	0.3
Peat briquettes	domestic	0.67	0.67	0.67
	industrial	0.134	0.134	0.134
Aviation gasoline	all	0.1	0.1	0.1
Jet fuel	all	1.0	1.0	1.0
Kerosene	all	0.03	0.03	0.03
Liquid petroleum gas	all	0.0002	0.0002	0.0002
Residual fuel oil	all	0.025	0.025	0.025
Motor gasoline	transport	0.15	0.15	0.03
Natural gas and other gases	combined	1.23*	1.23	1.23
	domestic	2.24	2.24	2.24
	industrial	0.216	0.216	0.216
		Submicron BC Emission Factors		
Hard coal, hard coal briquettes, coke oven coke, gas coke, brown coal coke	combined	1.58	0.82	0.46
	domestic	2.28	2.28	1.39
	industrial	1.10	0.298	0.149
Lignite brown coal, lignite briquettes	combined	2.84	1.48	0.82
	domestic	4.10	4.10	2.50
	industrial	1.98	0.536	0.268

BC, black carbon.

*Emission factors for natural gas and other gases are given in g TJ^{-1}. In order to convert emission factors of C from gC kg^{-1} gas to gC TJ^{-1} energy and volume densities of 19.3 kg TJ^{-1} [*Muhlbaier and Williams*, 1982] and 1.4 m^3 kg^{-1} were used.

Table 3b. Résumé of Emission Factors for Black Carbon Emission

Fuel Type	Emission Factors Found in Literature	Average Emission Factor
Hard coal (domestic)	4.55 a, 1 b	2.78
Hard coal (industrial)	0.325 a, 0.1 b, 0.075 c,d, 0.3 e	0.2
Diesel (traffic)	1.268-1.62 g, 0.5-5 h, 2.1 i, 3.4 j, 1-3 b, 0.3-2 e	2
Aviation gasoline	0.04 g, 0.1-0.3 b, 1-6 e	0.1
Jet fuel	1.13 g, 1.26 c, 0.1-0.3 b, 1-6 e	1
Residual fuel oil	0.016-0.051 c, 0.013-0.021 g	0.025
Motor gasoline (traffic)	0.015-0.048 g, 0.3 k, 0.011-0.014 j, 0.004-1 m, 0.007-0.4 e	0.03
Natural gas (domestic)*	5.8 b,j, 0.11 c,j, 0.12-1.54 e,j	2.24
Natural gas (industrial)	0.58 b,j, 0.055 c,j, 0.007-0.02 e,j	0.216
Hard coal (submicron industrial)	0.36 d, 0.176 f	0.298

Here, a, *Ball* [1987]; b, *Turco* [1983]; c, *Bocola and Cirillo* [1989]; d, *EPA* [1996]; e, *Hansen et al.* [1989]; f, *McElroy et al.* [1982]; g, *Cass et al.* [1982]; h, *Barbella et al.* [1988]; i, *Williams et al.* [1989b]; j, *Muhlbaier and Williams* [1982]; k, *Williams et al.* [1989a]; m, *Hansen and Rosen* [1990].

*Emission factors for natural gas and other gases are given in g TJ^{-1}.

found for BC and OC (Tables 3a and 4) give a ratio of 33:67. This ratio will be used to scale the emission factors of BC in order to calculate emission factors of OC for domestic usage of hard coal in semideveloped and underdeveloped regions of the world. However, as industrial processes tend to be more efficient, we will assume that the BC:OC ratio is 50:50 in all regions of the world.

For the submicron fraction of carbonaceous aerosol produced by uncontrolled industrial combustion of hard coal, we obtain an emission factor of 0.298 g kg^{-1} for both BC and OC, assuming that each of BC and OC comprise 25% of the submicron aerosol. The uncontrolled emission factor is assumed to be representative of submicron emissions for semideveloped countries. For developed countries we use the average characteristics of controlled processes for submicron particles to reduce the BC emission factor.

Lignite brown coal (or soft coal) has a lower calorific content than hard coal. The temperatures obtained in fires with lignite can be expected to be lower than those with hard coal. This lower temperature should lead to lower efficiency of burning and higher emissions. The *EPA* [1996] gives TPM emissions which are 1.8 times that of hard coal. We will therefore augment the BC emission factors of hard coal by a factor of 1.8 and use the ratio of *Rosen and Hansen* [1985] to calculate the emission factors for OC emissions from the combustion of lignite brown coal in all cases.

2.4.2. Diesel. For diesel the majority of emission factor data refers to vehicular use, and we replace the combined usage sector by the traffic sector. A compilation of emission factors from this source (Table 3b and Figure 4) shows that diesel is a significant source of carbonaceous aerosol. For traffic, BC is the most important fraction and comprises 55-79% of the carbonaceous aerosol [*Cass et al.*, 1982; *Muhlbaier and Williams*, 1982; *Lowenthal et al.*, 1994; *Guillemin et al.*, 1997] with the average fraction of BC being 66%. This implies that the emission factor for OC is a factor of 2 below the BC emission factor.

In a refinery an emission factor of 0.07 g kg^{-1} for use of distillate fuel was reported by *Cass et al.* [1982], and this value is assumed for industrial use of diesel. For industrial usage, *Lowenthal et al.* [1994] gives a ratio of 58:42 for BC:OC for stationary sources using distillate oil, which implies an emission factor of 0.05 gOC kg^{-1}. Domestic use of diesel is not well documented and is assumed to have the same emission factor and BC content as transport in developed countries.

2.5. Minor Sources of Carbonaceous Aerosol

Other fuels contribute emissions which may be important on a local or regional scale. We will now calculate their emission factors and assume that the sub-

Table 4. Emission Factors for Bulk Organic Carbon Aerosol.

Fuel Type	Sector	Underdeveloped, g kg^{-1}	Semideveloped, g kg^{-1}	Developed, g kg^{-1}
		Bulk OC Emission Factors		
Hard coal, hard coal	combined	3.09	1.76	1.08
briquettes, coke	domestic	9.54	9.54	5.83
oven coke, gas coke,	industrial	1.0	0.325	0.2
brown coal coke				
Lignite brown	combined	11.5	6.6	4.02
coal, lignite	domestic	24.5	24.5	15
briquettes	industrial	5.4	1.77	1.08
Peat	combined	2.71	2.71	2.71
Peat briquettes	domestic	6.07	6.07	6.07
	industrial	1.21	1.21	1.21
Diesel	transport	5.0	5.0	1.0
	domestic	1.0	1.0	1.0
	industrial	0.25	0.07	0.05
Aviation gasoline	all	1.15	1.15	1.15
Jet fuel	all	0.45	0.45	0.45
Kerosene	all	0.022	0.022	0.022
Liquid petroleum gas	all	0.02	0.02	0.02
Residual fuel oil	all	0.1	0.1	0.1
Motor gasoline	all	0.73	0.73	0.07
Natural gas and	combined	2.2	2.2	2.2
other gases*	domestic	11.2	11.2	11.2
	industrial	0.432	0.432	0.432
		Submicron OC Emission Factors		
Hard coal, hard coal	combined	2.29	1.19	0.66
briquettes, Coke	domestic	4.77	4.77	2.92
oven coke, gas coke,	industrial	1.10	0.298	0.149
brown coal coke				
Lignite brown	combined	8.55	4.45	2.46
coal, lignite	domestic	12.3	12.3	7.5
briquettes	industrial	5.94	1.61	0.804

OC, organic carbon.

*Emission factors for natural gas and other gases are given in g TJ^{-1}. In order to convert emission factors of C from gC kg^{-1} gas to gC TJ^{-1} energy and volume densities of 19.3 kg TJ^{-1} [*Muhlbaier and Williams*, 1982] and 1.4 m^3 kg^{-1} were used.

micron fraction of the emissions is similar to coal and diesel for solid and liquid fuels, respectively.

2.5.1. Solid Fuels. Hard coal briquettes are formed by compressing the fines from coal into a regular shape. Coke is a "solid product obtained from carbonisation of coal at high temperatures" [*United Nations*, 1993]. *Bocola and Cirillo* [1989] quote the same TPM emission factors for coke burning as that of hard coal. We therefore assume that carbonaceous emissions for these solid fuel types are the same as that of hard coal.

Peat is a fuel used in several countries although its global usage is quite small. Because of the low degree of maturation of this fuel, we will assume that emissions from domestic burning of peat are similar to that of wood. An emission factor of 12.3 gTPM kg^{-1} from *Liousse et al.* [1996] with a carbonaceous fraction of 55% [*Muhlbaier and Williams*, 1982] is assumed. We will assume that industrial processes are more efficient and have emission factors which are a factor of 5 lower. Because of the incomplete combustion of peat and low temperature in both industrial and domestic processes, we will assume that a small fraction (10%) of the carbonaceous aerosol is BC as in smouldering combustion of biomass burning [*Cachier et al.*, 1996]. Particles are also assumed to be in the submicron size range as for biomass-burning aerosol.

2.5.2. Liquid Fuels. Motor gasoline is a widely used fuel. A résumé of the emission factors used in calculating the average emission factor is given in Table 3b. For this fuel, as for diesel, the combined emission factor has been replaced by a traffic emission factor. An average of these figures leads to an emission factor of 0.03 gBC kg^{-1} which is 2 orders of magnitude lower than for diesel vehicles. The emission factors reported above were measured in developed countries so the average emission factor is representative only of developed regions. It would appear that the BC:OC ratio is lower (17:83) for noncatalytic cars than for catalytic cars (31:69) [*Cass et al.*, 1982; *Muhlbaier and Williams*, 1982] . We will assume an average of these ratios for developed countries while assuming that less developed countries are represented by noncatalytic cars. Domestic and industrial use of the fuel within a country is assumed to be similar to traffic.

For the following fuel types no sectorization is made between level of development or combustion process within a country. Kerosene is another fraction of the distillate oil. *Bocola and Cirillo* [1989] give a TPM emission factor of 0.35 gTPM kg^{-1} for kerosene. *Cass et al.* [1982] show that 14.6% of TPM from distillate oil is carbonaceous. We will assume that the breakdown of the BC:OC (58:42) is the same as for the industrial use of diesel.

There are very few emission factors for residual fuel oil. These are shown in Table 3b. The BC fraction of the emissions (20%) [*Cass et al.*, 1982] appears quite low.

There are also very few emission factors for liquid petroleum fuel. *Cass et al.* [1982] report TPM emission factors of 0.348 gTPM kg^{-1} and that 6% of the TPM is carbon, all of which is organic. *Bocola and Cirillo* [1989] report a lower TPM emission factor of 0.06 gTPM kg^{-1}. Taking the emission data of *Cass et al.* [1982] and assuming an emission factor for BC that is 1% of OC, we derive emission factors of 0.0002 gBC kg^{-1} and 0.02 gOC kg^{-1}.

For aviation, two types of fuel have to be considered. Aviation gasoline is intended for use in aviation piston power units only while jet fuel is needed for aircraft which utilize jet engines. For aviation gasoline we will assume here the median emission factor of the data set of 0.1 gBC kg^{-1}. According to *Cass et al.* [1982], BC comprises 8% of the carbonaceous aerosol emitted by aircraft. We therefore deduce an emission factor for OC of 1.15 gOC kg^{-1}. Emission factors for BC and OC have also been calculated for jet fuel [*Cass et al.*, 1982; *Turco*, 1983; *Bocola and Cirillo*, 1989; *Hansen et al.*, 1989]. If we use the BC:OC ratio obtained above for diesel to partition carbonaceous aerosol [*Cass et al.*, 1982], then we arrive at an emission factor of 0.5 gOC kg^{-1} for jet fuel.

2.5.3. Gaseous Fuels. There are also several types of gaseous fuel included in the United Nations fuel database. Natural gas is by far the largest of these fuel types, so we will approximate the emissions of these fuel types by the emission factors for natural gas. It is also convenient to do this as natural gas is the most studied gaseous fuel. The emission factors are, however, particularly low (Table 3b).

3. Sensitivity of Emissions to Assumed Emission Factors

Recent measurements of the emission of submicron light-absorbing particles from a lignite power plant [*Bond et al.*, 1998] suggest a possible emission factor of 0.05 g kg^{-1}, which is a factor 6.5 lower than that assumed here. However, as these data became available after we had finished our computations for the global distributions discussed later, we have not included these data in our inventory. However, we can calculate what effect this lower emission factor would have for BC. The global emission of BC is 2.14 TgBC from hard coal and 0.7 TgBC from lignite. If the emission factor found by *Bond et al.* [1998] is more representative of the correct emission, then these figures would decrease to 0.33 TgBC and 0.11 TgBC, respectively. The global emission would therefore decrease by 2.4 TgBC, or close to 50%.

For diesel fuel, there is a range of a factor of 4 in the emission factors in Table 3b. The global emission from diesel is calculated to be 1.71 TgBC, so this could range from 0.86 to 3.42 TgBC.

One can say that the emission of BC, and therefore also of OC, is uncertain to at least a factor of 2 and may well be overestimated. Measurements of emission factors under the appropriate operating conditions are vital if this uncertainty is to be reduced. Other sensitivity studies may need to be made with regard the lifetime of the hydrophobic aerosol, but these studies are beyond the scope of this work.

4. Comparison With Other Emission Data Sets for Carbonaceous Aerosol

The total emission based on bulk emission factors is 10.1 TgOC yr^{-1} and 6.4 TgBC yr^{-1}. The total emission based on submicron emission factors is 7.0 TgOC yr^{-1} and 5.1 TgBC yr^{-1}. The effect of allowing only for the submicron fraction of aerosol is to decrease the global emissions of BC by about 20%. For OC this effect is to reduce the total emissions by 33%. The difference in reductions is due to the greater importance of the organic fraction in coal emissions.

For both components the most important area for emissions appears to be the non-USSR area of the Asian continent, which accounts for 35-40% of the global emissions. The European Union and North American countries have similar emissions (7-9% and 6-10%). The global distribution of submicron emissions of BC and OC are shown in Figures 2 and 3. The fractional contribution of coal (hard and soft), vehicular (diesel and motor gasoline), and other fuel types to bulk and submicron carbonaceous aerosol emission is shown in Figure 4. One can see that the combustion of coal dominates the global emission of carbonaceous aerosol, even for submicron aerosol. This may be important for future emission scenarios as developing countries, especially China, use this fuel to create the power needed by their growing industry. This also emphasizes the need for more accurate evaluation of emission factors for this fuel.

The only detailed fossil fuel global BC emission data sets which have been published are those of *Cooke and Wilson* [1996] and *Penner et al.* [1993]. There is a 20% difference in the totals of the two papers because of differences in the fuels used in compiling the data sets and some discrepancies in the evaluation of emission factors. Both of them are based on fuel usage and bulk emission factors but did not explicitly take into account emission controls or combustion efficiency. One can therefore expect that in the work presented here bulk emissions for developed regions will be lower and for developing regions will be similar or higher. Our revised inventory results in a global decrease of 20% in BC emission when compared to *Cooke and Wilson* [1996] but is similar to *Penner et al.* [1993].

Table 5a shows the regional breakdown of the two BC emission data sets developed in this work. It must be emphasized that in our work the contribution to global BC emissions from South and Central America can be attributed mainly to the use of diesel fuel in these countries.

Table 5a also compares the regional breakdown of the two BC emission data sets developed here to those of *Cooke and Wilson* [1996] and *Penner et al.* [1993].When compared to the *Cooke and Wilson* [1996] data set the largest decreases in bulk BC emissions are for eastern Europe and the former USSR with decreases of 30% in each area. The emissions from western Europe and North America have decreased by 50%, and this is primarily due to the differentiation between industrialized and nonindustrialized countries. In addition, account has been taken of emission controls in the developed countries.

The apparent good agreement between the emissions for China is, in fact, a coincidence as there was an overestimation of the industrial and underestimation of the domestic fraction of consumption of coal in China in the *Cooke and Wilson* [1996] paper, where the emissions should have been estimated to be higher.

When compared to the *Penner et al.* [1993] data set, the emissions for western Europe and North America are somewhat higher. The main differences are in China and the former USSR, where our estimates are lower. In Africa, South and Central America, and the rest of Asia the emission of BC is quite a bit higher than in the work of *Penner et al.* [1993] because of the higher emission factor for diesel in these regions.

There are also large differences in the fuel use inventories used. A calculation using the emission factors of *Penner et al.* [1993] and the fuel usage data set (coal and diesel only) used in this work resulted in a global emission of 9.6 TgBC. The 45% discrepancy should not

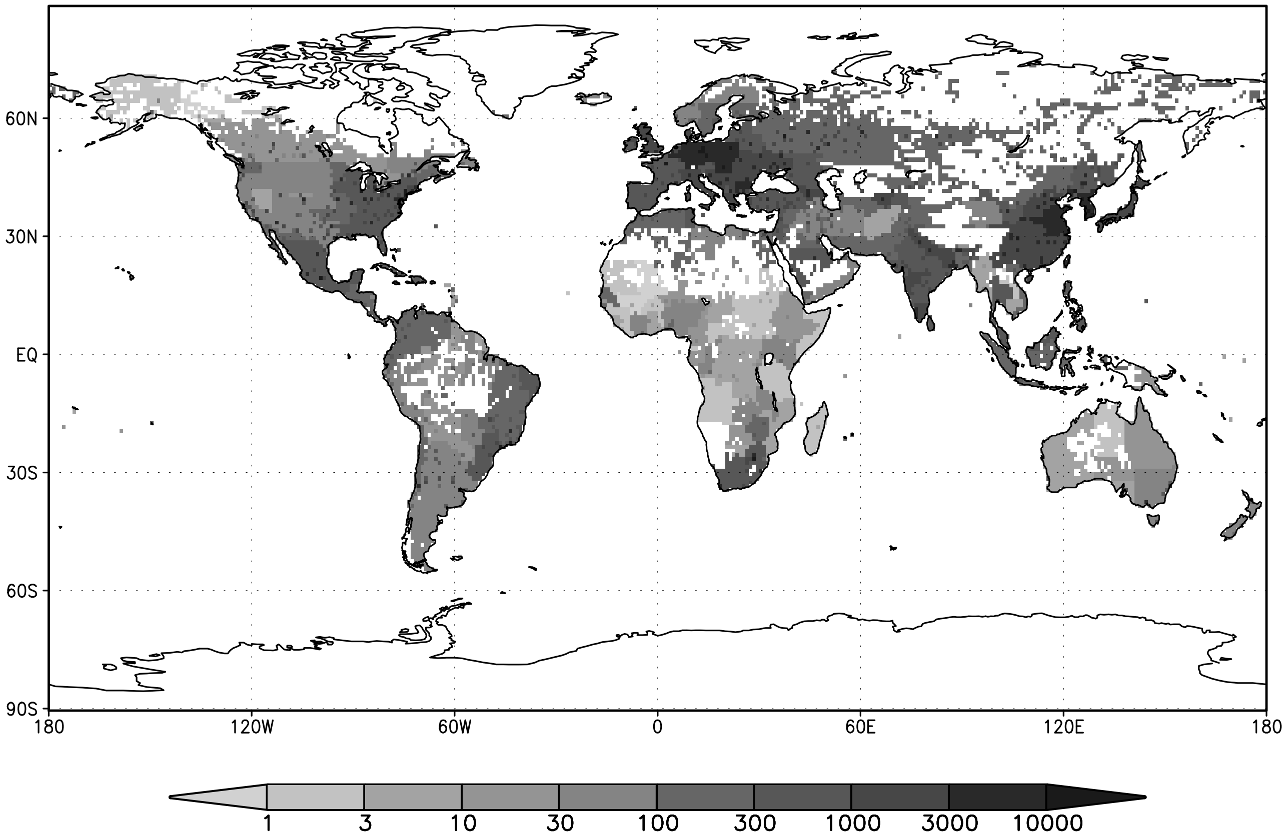

Figure 2. Global distribution of black carbon (BC) emissions on a 1° × 1° scale.

Table 5a. Comparison With *Cooke and Wilson* [1996] and *Penner et al.* [1993] of Fossil Fuel Black Carbon Emissions by Region

Country or Region	This Work Bulk	This Work Submicron	*Cooke and Wilson* [1996] Bulk	*Penner et al.* [1993] Bulk
European Union 15	0.55	0.47	1.09	0.47
Other western Europe	0.14	0.11	...	...
Eastern Europe	1.05	0.68	1.56	1.50
Africa	0.20	0.17	0.34	0.04
South America	0.26	0.26	0.10	0.02
Central America	0.12	0.12	0.01	0.0
North America	0.55	0.49	1.27	0.32
Oceania	0.04	0.03	0.10	0.02
Former USSR	1.07	0.69	1.55	1.69
China	1.46	1.15	1.10	2.16
Rest of Asia	0.95	0.89	0.85	0.37
Total	6.39	5.06	7.97	6.64

Emissions are in TgBC yr^{-1}

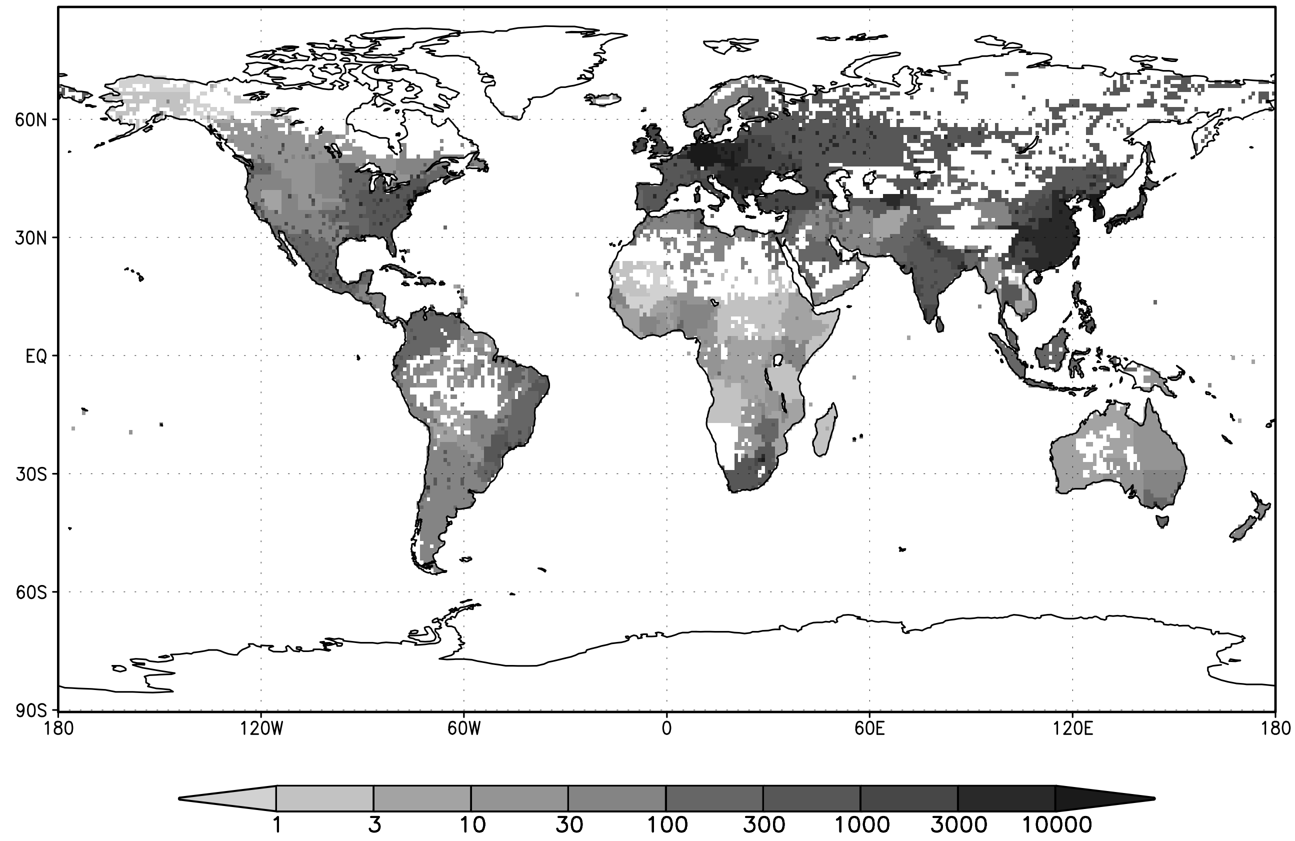

Figure 3. Global distribution of organic carbon (OC) emissions on a 1° × 1° scale.

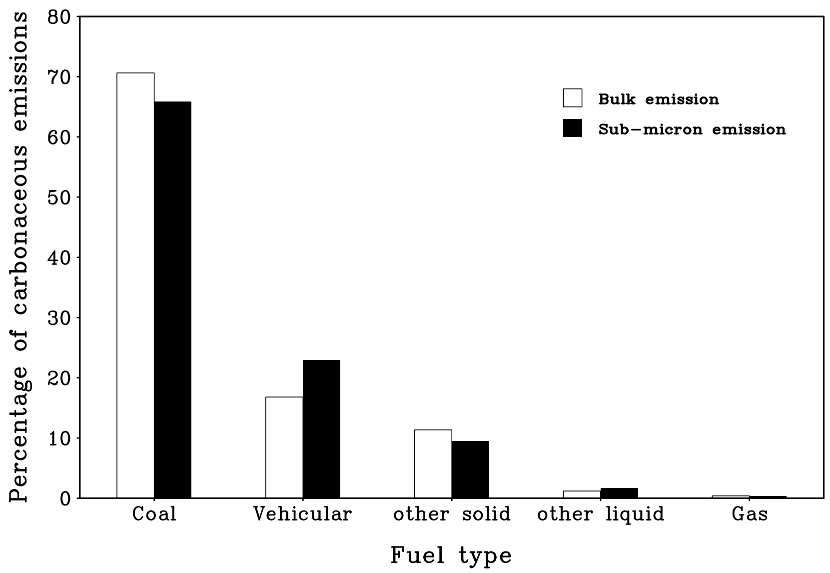

Figure 4. Relative contribution of various sources to global carbonaceous aerosol emission.

be due to the different years for which emissions were calculated.

Since only the emission factors of the coal-like fuels have been reduced in order to estimate the submicron emission of carbonaceous aerosol, one can expect the differences between the bulk- and submicron-based emissions to be greatest in areas where coal combustion is most important. The regional emission of BC indeed decreases in eastern Europe (35%), the former USSR (35%) and China (20%) when only submicron emissions are considered.

The regional breakdown of the emission of primary organic aerosol is shown in Table 5b. As far as we are aware, there has been only one other estimate of the emission of OC aerosol from the combustion of fossil fuel. *Liousse et al.* [1996] estimated the global organic carbon aerosol emission by multiplying the coal and diesel fraction of the fuel use BC inventory of *Penner et al.* [1993] by the ratio of OC to BC (3.1:1) as measured in urban situations, resulting in a global total emission of 20.35 TgOC. This method is reasonable but certainly takes into account the local and rapid secondary production of anthropogenic organic aerosol which leads to a higher ambient concentration of organic aerosol. Following the method of *Liousse et al.* [1996], the total presented here suggests that primary organic aerosol (10.1 TgOC) emitted from the combustion of fossil fuel may account only for approximately one half of the total anthropogenic organic aerosol (6.4 TgBC x 3.1 = 19.8 TgOC) in source areas.

5. Implementation of Carbonaceous Aerosols in ECHAM

5.1. Meteorological Model

In this study we used the fourth generation Max-Planck-Institute model, ECHAM4, which is the most recent in a series evolving from the European Centre for Medium-Range Weather Forecasts (ECMWF) model. As with the previous ECHAM versions [*Roeckner et al.*, 1992, 1996], ECHAM4 is based on the primitive equations. Prognostic variables are vorticity, divergence, surface pressure, temperature, water vapor, cloud water, and chemical species. Except for the water components and the chemical species, the prognostic variables are represented by spherical harmonics with triangular truncation at wavenumber 30 (T30). Advection of water vapour, cloud water and chemical species is treated with a semi-Lagrangian scheme [*Williamson and Rasch*, 1989]. A semi-implicit time-stepping scheme is employed with a weak time filter. The time step is 30 min for dynamics and physics, except for radiation, which is calculated at 2-hour intervals. A hybrid sigma-pressure coordinate system is used with 19 irregularly spaced levels up to a pressure level of 10 hPa. The radiation code has been adopted from the ECMWF model [*Morcrette*, 1991] with a few modifications such as the consideration of additional greenhouse gases (methane, nitrous oxide, and 16 CFCs) and various types of generic aerosols. The radiation code has two spectral intervals in the shortwave and six in the longwave and is similar to that used by *Boucher and Anderson* [1995]. The shortwave part of the ECMWF code, developed by *Fouquart and Bonnel* [1980], solves the radiative transfer equation by integrating the fluxes between 0.2 and 4 μm. Solar radiation is attenuated by absorbing gases (mainly, water vapor, carbon dioxide, oxygen and ozone) and scattered by molecules, aerosol, and cloud particles. For the spectral integration the scheme considers two intervals, one for the visible (0.2-0.68 μm) and one for the near-infrared (0.68-4 μm). The cutoff at 0.68 μm makes the scheme computationally efficient, inasmuch as interactions between gaseous absorption and scattering processes are accounted for only in the near-infrared interval. Optical properties of aerosol particles are calculated from Mie theory [*Koepke et al.*, 1997] and adapted to the broadband model [I. Schult and R. van Dorland, personal communication, 1996]. Fractional cloud cover is parameterized as a function of relative humidity [*Roeckner*, 1995; *Sundqvist*, 1978]. ECHAM has been extensively applied and validated in climate studies [*Cess et al.*, 1990; *Latif et al.*, 1990; *Lohmann and Roeckner*, 1995; *Lohmann et al.*, 1995; *Bengtsson et al.*, 1996; *Wild et al.*, 1996].

Transport, dry, and wet deposition of aerosol particles are calculated on-line in the model. Advective transport of aerosols as well as vertical exchange in the boundary layer and in convective clouds are handled in the same way as the transport of water vapor. The performance of this scheme was successfully tested using the aerosol-like radionuclides lead-210 and beryllium-7 [*Brost et al.*, 1991; *Feichter et al.*, 1991]. However, there appear to be some problems with the transport in the Arctic region as mass concentrations of these aerosols were underpredicted by the model.

5.2. Implementation of Carbonaceous Aerosol in ECHAM

The emissions of carbonaceous aerosol were transformed from the $1^\circ \times 1^\circ$ resolution to the T30 resolution ($\sim 3.75^\circ \times 3.75^\circ$) by allocating the appropriate fraction of each emission grid cell to the appropriate

Table 5b. Comparison With *Liousse et al.* [1996] of Fossil Fuel Organic Carbon Emissions

Country or Region	This Work Bulk	This Work Submicron	*Liousse et al.* [1996] Bulk
European Union 15	0.68	0.51	···
Other western Europe	0.28	0.17	···
Eastern Europe	2.68	1.68	···
Africa	0.24	0.17	···
South America	0.17	0.17	···
Central America	0.08	0.08	···
North America	0.48	0.39	···
Oceania	0.06	0.05	···
Former USSR	2.19	1.35	···
China	2.23	1.54	···
Rest of Asia	1.04	0.90	···
Total	10.12	7.01	23.75

Emissions are in TgOC yr^{-1}

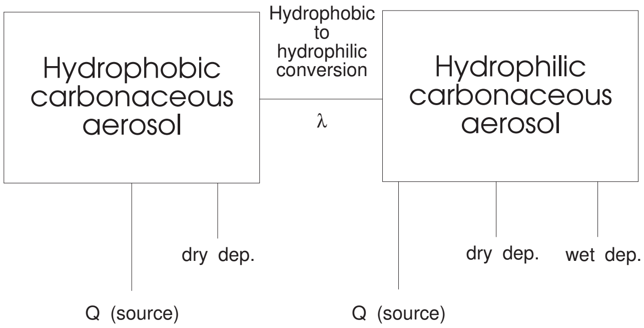

Figure 5. Emission and transformation scheme for carbonaceous aerosol.

T30 resolution ECHAM grid cell.

The aerosol module used to model the carbonaceous aerosol is based on that used for BC particles by *Cooke and Wilson* [1996]. The scheme is shown schematically in Figure 5. The aerosol model now allows for emission of both hydrophobic and hydrophilic aerosol as opposed to only hydrophobic emissions in the work of *Cooke and Wilson* [1996].

Particulate carbon is predominantly hydrophobic, but a certain fraction of the emissions may be hydrophilic [*Cachier*, 1998]. Black and organic carbon both have various compounds attached to the surface [*Smith et al.*, 1989] which may determine their atmospheric behavior and also allow a chemical change in the properties of the surface layer as it ages in the atmosphere. Emissions of BC are assumed to be 80% hydrophobic. We assume that OC is emitted in equal proportions of hydrophobic and hydrophilic aerosol. The aging process for both BC and OC is represented by a transfer of hydrophobic to hydrophilic aerosol with an exponential lifetime of 1.15 days. The aerosol lifetime is assumed to be governed by wet and dry deposition, and no chemical sinks are used in this work. In-cloud scavenging and subsequent removal of hydrophilic carbon by precipitation is calculated explicitly in terms of the models local precipitation formation rate [*Feichter et al.*, 1991]. The dry deposition flux to the ground is assumed to be proportional to both the concentration in the lowest model layer (30 m above ground) and to a prescribed dry deposition velocity. For hydrophilic carbonaceous aerosol this is assumed to be 0.025 cm s^{-1} over dry surfaces and 0.2 cm s^{-1} over wetted surfaces and melting snow or ice [*Ganzeveld et al.*, 1998]. Hydrophobic aerosols are deposited by a constant velocity of 0.025 cm s^{-1} as the hydrophobic aerosols are assumed not to be influenced by wetted surfaces.

6. Comparison of the Carbonaceous Model With Measured Data

As we are interested in the global distribution of carbonaceous aerosol we will implement the submicron emission fields described above. The use of the submicron emissions implies that the results of this simulation may tend to be lower than the measurements, at least close to the source regions. A spin-up period of 3 months was allowed so that the atmospheric concentrations of carbonaceous aerosol would reach equilibrium. The model was then run for a further 5 years,

Table 6. Atmospheric Burdens and Lifetimes of the Carbonaceous Aerosol

Species	Burden, Tg	Lifetime, days
BC (this work)	0.073	5.29
BC (FF, CW96)	0.17	7.85
BC (FF, L96)	0.070	3.86
OC (this work)	0.087	4.54
OC (FF, L96)	0.232	3.86

CW96, *Cooke and Wilson* [1996]; L96, *Liousse et al.* [1996]; FF, fossil fuel component of the burden, assuming that the lifetime of BC from fossil fuel and biomass burning are identical.

and monthly means over this 5-year period are compared with measurements in the following sections. The annual average atmospheric burden and lifetimes of the carbonaceous aerosols are given in Table 6. These are typical lifetimes for fine atmospheric hydrophilic particles with the lifetime of sulphate aerosol being similar to that of OC.

The burden found here compares well with that of *Liousse et al.* [1996] (0.077 TgBC due to fossil fuel BC, assuming that the lifetime of fossil fuel and biomass burning BC are similar). The burden of *Cooke and Wilson* [1996] (0.17 TgBC due to fossil fuel BC) is much higher. This is due to the emission scheme used in this work, which emits less hydrophobic aerosol and thus shortens the lifetime of the aerosol. The overall burden of BC can be expected to be approximately 0.15-0.25 TgBC, depending on the lifetime of the aerosol when biomass burning BC is included. The OC burden can be compared to that of *Liousse et al.* [1996] (0.237 TgOC due to fossil fuel OC). The difference in the burdens can be attributed to the emissions as the ratio of the burdens is quite similar to that of the emissions. The overall anthropogenic burden of OC is difficult to quantify from the present study but may be of the order of 1 TgOC when biomass-burning emission and secondary production of OC is accounted for.

We will now make a comparison between the modeled and measured values of BC and OC at various sites around the globe. We will make only comparisons with measurements made in the Northern Hemisphere as this is where the majority (94% of our inventory) of fossil fuel emissions occur. The validation of the model requires that the model reproduce the measured concentrations of BC and OC in both air and precipitation.

6.1. Comparison of Modeled Concentrations of Black Carbon With Measurements.

6.1.1. Comparison of average of measurements and model of BC for long-term sites. The ECHAM model reports information on the wind direction for each of the grid points of the model output on a 12 hourly basis. The model wind direction data, when combined with the modeled carbon aerosol mass concentrations, allow one to calculate sectored averages for various sites. This is quite useful as measurements at various sites are often made using a sectored approach. This means that measurements are used in calculating a monthly average only if various conditions are fulfilled. Normally, the main condition is that the wind direction is such that possible local pollution is excluded and air masses which have traversed over a "clean sector" are the only ones to be measured. The ability of the model to reproduce these sectored conditions places greater reliability on the comparison between the model and measurements.

Long-term measurements of BC tend to be inferred from absorption measurements using a constant absorption cross section. However, *Liousse et al.* [1993] found that the absorption cross section of BC varied by a factor 4 as one moves from source to remote regions. This variation may cause some problems in evaluating the actual BC mass concentrations, especially at remote sites. It should also be remembered that there are inherent difficulties in the measurement of BC or light absorption coefficients [*Heintzenberg et al.*, 1997], which may account for some of the discrepancies seen in the comparison. The model monthly geometric means are calculated initially for the 5-year run and are then averaged to obtain the statistics shown in Figures 6, 7, 8, and 9. The geometric deviation is therefore a measure of the interannual variability of the monthly mean. The measured data are treated in the same manner in Figures 6 and 7.

A 7-year average of the measurements from the data of *Cooke et al.* [1997] for BC measurements at Mace Head, Ireland has been used to compare with the model. The comparison between the modeled and measured values of BC mass concentrations are shown in Figure 6; the monthly means are for air masses where the wind direction was from the marine sector. The geometric deviations are also shown. The model results are well within 1 geometric deviation of the measurements, except for July and August, where the model overpredicts the measured concentrations by a factor of 2. This may be due to three causes: 1) the emissions being put into the model being incorrect at this time of year, 2) the

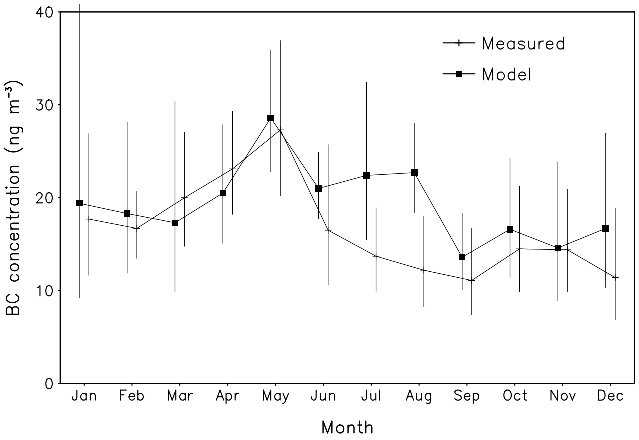

Figure 6. Comparison of modeled and measured black carbon at Mace Head for the marine sector. Geometric deviations of the monthly means over the measured and modeled periods are shown.

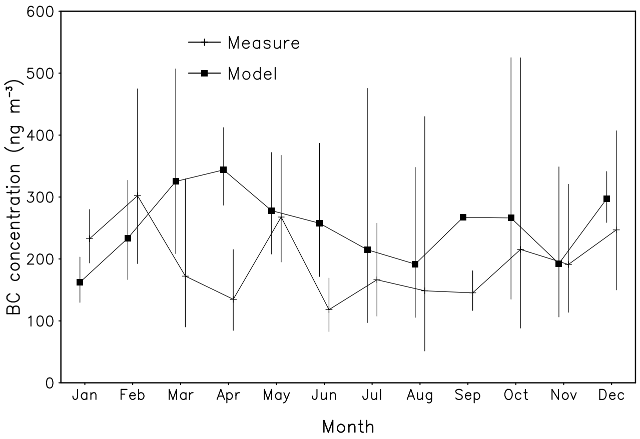

Figure 7. Comparison of modeled and measured black carbon at Mace Head for the continental sector. Geometric deviations of the monthly means over the measured and modeled periods are shown.

model representing the transformation of hydrophobic to hydrophilic BC being incorrect, or 3) influence of European air masses in the marine sector. The seasonality of the emissions are taken from *Rotty* [1987] and a much stronger seasonality would be needed in order to decrease the summer concentrations by 30-40%, which is unrealistic for fossil fuel derived combustion. The possibility that the fixed transformation rate between hydrophobic and hydrophilic carbon aerosol used in this model is not correct must therefore be raised. The transformation of carbonaceous aerosol from hydrophobic to hydrophilic is meant primarily to represent the coating of hydrophobic carbon aerosol with more hydrophilic species. During the summer months, photochemical oxidation processes may modify this coating. This would then generally lead to a more hydrophilic aerosol, which would be more easily wet-deposited in the summer months, and a decrease in the mass concentration. Another point which can also be raised is the occasional occurrence of air masses which have been transported from the European continent but then arrive at Mace Head from a westerly direction. These air masses will increase the average mass concentration. Indeed, *Cooke et al.* [1997] show that a simple sectoring of the measurements with respect to wind direction is not sufficient in excluding air masses which have recently been influenced by anthropogenic source regions and may explain some of the discrepancies between the model and the measurements.

We can also compare the modeled and measured mass concentration where the air masses are relatively recently influenced by emission sources. Air masses which have passed over the European continent are directly transported to Mace Head within 1 or 2 days, generally. The monthly means for BC mass concentration when the wind direction is between 45° and 135° (easterly sector) are shown in Figure 7. The model generally overestimates the BC mass throughout the year although the modeled results are almost always within 1 geometric deviation of the measured mass concentrations. Some of this discrepancy may be due to the grid box immediately to the east of that containing Mace Head extending as far as the east coast of Ireland, where the emissions are much higher than the Irish average. This would mean that the transport time for these emissions would be shortened as emissions are smoothed over the entire grid box.

Black carbon optical measurements made at Barrow, Alaska, during 1989 [*Bodhaine*, 1995] are compared with the modeled values of BC at the surface in Figure 8. The model underpredicts throughout the year although agreement in the summer period is more reasonable. The peak in the measurements, which may be attributed to Arctic haze events, is not well represented in the model. This has also been noticed for a comparison between modeled and measured sulphate aerosol in the Arctic [*Feichter et al.*, 1997] and suggests that there is a problem in the ECHAM model with the transport and removal in this area. Transport in stratified layers occurs frequently in spring. For example, layers of BC have been observed during this time period [*Rosen and Hansen*, 1984], and transport in these layers would not

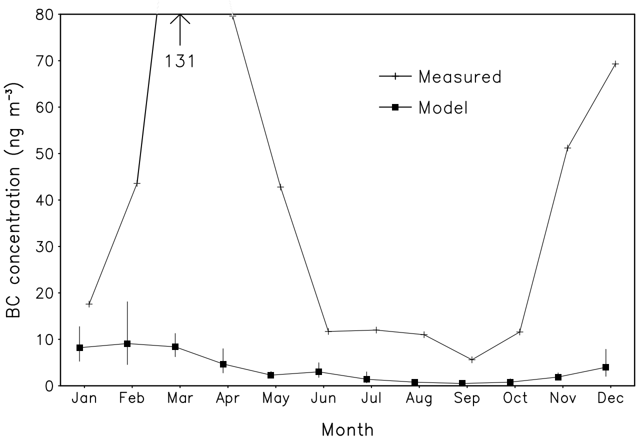

Figure 8. Comparison of modeled and measured black carbon at Barrow. Geometric deviations of the monthly means over the modeled period are shown.

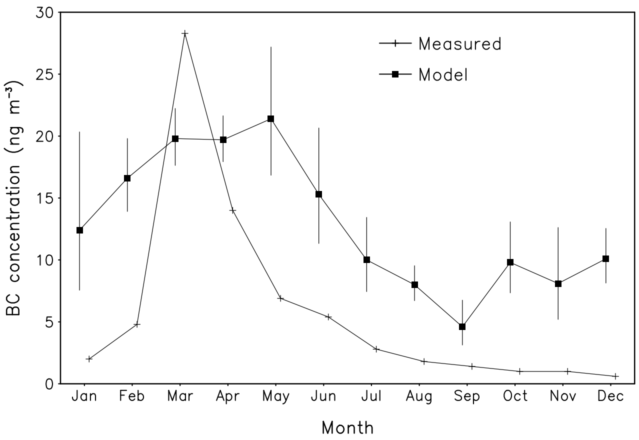

Figure 9. Comparison of modeled and measured black carbon at Mauna Loa. Geometric deviations of the monthly means over the modeled period are shown.

be well represented in the ECHAM model. The underprediction of the BC mass concentration in summer may also indicate that vegetation fires in the boreal region need to be taken into account, as suggested in recent studies in Greenland cores [*Legrand et al.*, 1992].

For Mauna Loa, Hawaii, BC data [*Bodhaine*, 1995] are compared in Figure 9 to the modeled values of BC. The modeled values are from the layer in the model corresponding to the height of the station at Mauna Loa. In this case the model overpredicts the measurements for most of the year although the magnitudes of both are similar. The seasonalities of the modeled and measured BC concentrations are reasonably similar in that there are higher BC mass concentrations in the first 6 months of the year.

6.1.2. Comparison of point measurements of BC. There have been many measurements of BC for time periods of several days to several years. A compendium of these measurements is given in Table 7 along with the modeled concentrations over the appropriate time period. The modeled concentrations are the range of the monthly means over the time period involved. In general, the modeled and measured mass concentrations of BC at remote or marine sites are in very good agreement or are slightly underestimated.

Measurements made in urban areas will be representative of the area where there is a large population density. Therefore the measurements of BC should be generally higher than the model. This is true for most of the urban sites. Some tendencies are reproduced in the modeled concentrations, such as the north to south gradient in the measurements over Germany.

For the rural sites, there appear to be two regimes where the modeled concentrations are either much higher or much lower than the measured values. These discrepancies may be explained if one looks at the regional sources of BC near these sources, and the sites may not be representative of the entire grid box in which they are located. The sites where the modeled concentrations are high (as in China and Hungary) are generally in large source areas, so it may be expected that there will be a large area with high modeled mass concentrations near the surface. The sites where the modeled concentrations are lower (such as the French and Dutch sites) are generally situated in areas where emissions are less important.

6.1.3. Comparison of measurements and model in the vertical profile. Figure 10 gives a comparison between the data of *Hansen and Novakov* [1988], *Pueschel et al.* [1992], and *Blake and Kato* [1995] and the model for nonsurface measurements of BC. From the surface to approximately 6 km, there is reasonable agreement between the model and measured values of BC. At a height of approximately 10 km the model appears to overestimate the measured mass concentration by an order of magnitude. At higher altitudes the modeled BC mass concentrations are within, although at the upper end of, the limits of the measurements. It would appear that the model generally overestimates the mass concentration in the upper troposphere. This may indicate a problem with vertical transport in the model as the surface measurements of BC are in reasonable agreement with the measurements. It should be remembered, however, that the vertical profile measure-

Table 7. Comparison of Modeled and Measured Black Carbon Concentration at Various Sites Around the Globe.

Station	Latitude	Longitude	Concentration, ng m^{-3} Modeled	Measured	Time Period
			Remote/Marine sites: Model/Measured Ratio = 0.684		
Ny Alesund	79°N	12°E	3-11	70 (28-174) a	March-May
			5-11	293 (123-567)b	March-April
			1-5	2 (1.2 - 81) a	July - Sept.
Greenland	70°N	40°W	2.2	30.5 c	July
Böisto Island	60°20'N	26°30'E	312	50 - 1000 d	June
NE Atlantic			121-177	268 e	Oct.-Nov.
Corsica	42°N	9°E	485	380 f	spring
Oki Island	36°N	133°E	673	520 g	annual
Hachi-jima	33°5'N	139°45'E	241	1070 h	Jan.
			252	740 h	Dec.
Saint Nicholas Island	33°9'N	119°18'W	206-210	160 i	May-July
Bermuda	32°45'N	65°W	55	30 j	Feb.
			17	40 j	Aug.
East China Sea			246-353	133 - 505 k	April, Oct.-Dec.
Chichi-jima	27°N	142°E	121	610 h	Dec.
Sargasso Sea	27°N	72°W	40	135 l	
			Rural Sites: Model/Measured Ratio = 1.219		
East Arctic	79°33'N	90°37'E	13-17	25 - 115 m	March-April
Abisko	68°18'N	18°30'E	79-94	393 n	March-April
Landes forest	44°N	1°W	179-250	300 f	autumn
Cheboque Point	43°48'N	66°6'W	203-285	81 - 139 o	Aug.-Sept.
Abastumani	41°30'N	42°40'E	641	450-2850 p	
				600 q	
			652	980 r	July
Allegheny	40°N	79°W	762	1300 s	Aug.
Rörvik	57°18'N	12°12'E	300-788	725 t	Jan.-May
Petten	52°54'N	2°55'E	395	1631 u	April
Hemsby	52°24'N	1°24'E	530	104 v	annual
Gif sur Yvette	48°42'N	2°8'E	919 - 1078	1650 - 2750 f,w	seasonal
Senonche	48°34'N	12°E	573	1200 x	March
K Pustza	46°57'N	19°42'E	1731	810 y	annual
West Mountain	40°N	116°E	3193	1710 - 2610 k	Aug.
Lin'an	30°15'N	119°42'E	3647-3744	2070 k	July-Aug.

Table 7. (continued)

Station	Latitude	Longitude	Concentration, ng m^{-3} Modeled	Measured	Time Period
			Urban Sites: Model/Measured Ratio = 0.634		
Kurressare	58°15'N	22°30'E	343-804	500 - 1800 z	annual
Kap Arkona	57°37'N	13°21'E	545	400 aa	annual
Moscow	55°45'N	37°35'E	1397-1793	3500 - 6750 ab	summer,winter
Hamburg	53°52'N	9°59'E	2443	1975 y	annual
Leeds	53°48'N	1°34'W	416-674	780 - 1300 ac	summer-winter
Neuhaus	53°16'N	10°54'E	2443	500 aa	annual
Neuglobsow	53°6'N	12°52'E	2443	600 aa	annual
Potsdam	52°3'N	13°4'E	3706	1000 aa	annual
Arnhem	52°N	5°54'E	2334-2505	2950 ad	Oct.-Nov.
Halle	51°29'N	12°E	3706	1600 aa	annual
Gorlitz	51°10'N	14°59'E	4837	1300 aa	annual
Radebeul	51°6'N	13°55'E	4837	1400 aa	annual
Paris	48°50'N	2°20'E	1301	4600 w	annual
Vienna	48°12'N	16°22'E	1737	4330 u	March
Orleans	47°54'N	15°2'E	573	2900 ae	March
Clermont Ferrand	45°46'N	34°E	907	2400 ae	April
Kislovodsk	43°50'N	42°45'E	763 - 827	2170 - 5900 p	Sept.-Oct.
Dushanbe	38°33'N	68°48'E	1158 - 1374	10700 - 12000 af	Aug.-Sept.
Nagoya	35°10'N	136°50'E	673	13000 ag	annual
Los Angeles	34°4'N	118°15'W	902 - 1347	3400 ah	June-Sept.
Ecuador	2°15'S	79°52'W	164	100 - 520 l	June

The range in the modeled values is the range of the monthly modeled means for the same period as the measurements. Here, a, *Heintzenberg* [1982]; b, *Clarke* [1989]; c, *Pertuisot* [1997]; d, *Raunemaa et al.* [1993]; e, *O'Dowd et al.* [1993]; f, *Cachier et al.* [1989]; g, *Mukai et al.* [1990]; h, *Ohta and Okita* [1984]; i, *Larson et al.* [1989]; j, *Wolff et al.* [1986]; k, *Parungo et al.* [1994]; l, *Andreae et al.* [1984]; m, *Polissar* [1993]; n, *Noone and Clarke* [1988]; o, *Chýlek et al.* [1996]; p, *Lyubovtseva and Yatskovich* [1989]; q, *Clarke et al.* [1984]; r, *Dzubay et al.* [1984]; s, *Keeler et al.* [1990]; t, *Brorström-Lundén et al.* [1994]; u, *Berner et al.* [1996]; v, *Yaaqub et al.* [1991]; w, *Brémond et al.* [1989]; x, *Cachier et al.* [1990]; y, *Heintzenberg and Mészáros* [1985]; z, Ü. Kikas et al. (unpublished manuscript, 1997); aa, *Zier* [1991]; ab, *Kopeykin et al.* [1993]; ac, *Willison et al.* [1985]; ad, *Janssen et al.* [1997]; ae, *Del Delumyea and Kalivretenos* [1987]; af, *Hansen et al.* [1993]; ag, *Kadowaki* [1990]; ah, *Adams et al.* [1990].

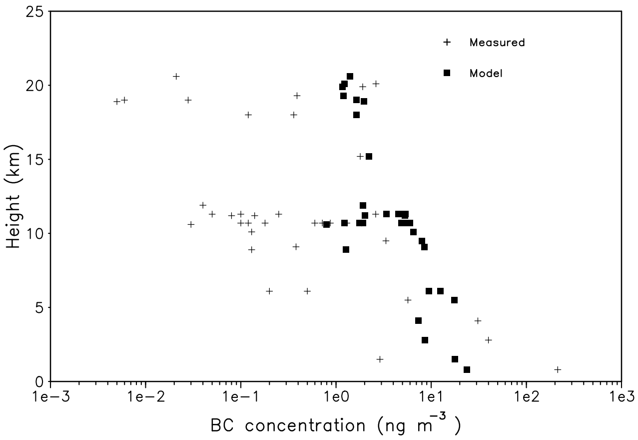

Figure 10. Comparison of BC vertical profile data.

ments are samples over very short time periods, while the modeled values are monthly means, and this may be responsible for some of the discrepancy.

6.1.4. Comparison of wet deposition of BC. Wet deposition is the most efficient sink for submicron aerosol in the atmosphere. A test of the model implemented here is to replicate the concentrations of BC in precipitation. A comparison of modeled and measured wet deposition of BC is made in Table 8. The model underestimates (5-93%) the wet deposition in all regions where measurements have been made. The disagreement between the model and measurements appears to be worst in the Arctic region. This may be due to an additional problem of the model, the weak transport in this region, as discussed in the section on mass concentrations of BC in air at Barrow. For Mace Head the modeled values are an average over 5 years, and the maximum monthly mean for the period for October or November is 30 μg L^{-1}. We can therefore argue that the measurements performed during a short campaign (31 μg L^{-1}) may have been influenced by European airmasses.

Hurricane Hill on the west coast of the United States is quite close to Seattle, so the data of *Ogren et al.* [1984] allow us to see the influence of urban areas on measurements of BC in precipitation. The agreement between the model and measurement at Hurricane Hill is very good, while the model underpredicts the wet deposition in Seattle by a factor of 5. The importance of BC in rainfall in source regions, such as at Gif sur Yvette and Seattle, is additional evidence that BC is not completely hydrophobic when emitted.

6.2. Comparison of Modeled Concentrations of Organic Carbon With Measurements

It is very difficult to compare the modeled mass concentrations of OC from fossil fuel sources with measurements. This is partly due to the fact that there are other sources of OC aerosol. There are natural sources of aerosol organic substances as well as secondary production of aerosol from gaseous emissions from natural and anthropogenic sources. In any case, data are sparse and there are few long-term measurements of OC.

6.2.1. Comparison of point measurements of OC. The modeled and measured concentrations of OC at various points in the Northern Hemisphere are shown in Table 9. The modeled concentrations of OC for marine sites is greatly underestimated. This is not surprising as aerosol from secondary and/or natural sources may be expected to dominate in remote regions. For the "rural" sites the disagreement between the modeled and measured OC concentrations is similar to the ratio between the modeled and measured OC for the rural and marine sites of the order of 0.17. However, for the same areas the average measured to modeled ratio for BC is close to unity. This would imply that rather than being a problem with the inventory, the disagreement originates from the addition of OC en route from secondary production and natural sources. These additional sources increase the concentration of particulate OC by a factor of 4-5, if the BC and OC measurements are reliable.

The ratio of modeled to measured OC in urban areas is approximately 0.33. One can perhaps estimate the contribution of sub-grid-scale secondary production of OC in source regions by looking at the ratio of the modeled and measured concentrations. However, as mentioned earlier, the grid size of the model will cause an underestimation of the concentrations in source areas. For BC the modeled to measured ratio is 0.63. If the OC ratio is corrected for this effect, this leads to a ratio of modeled to measured OC of 0.52. This value supports the assessment made earlier (section 4) that primary OC may account for only about 50% of total particulate OC in source regions.

6.2.2. Comparison of wet deposition of OC. There are few measurements of wet deposition of OC. One must be careful when comparing measurements of OC deposition as most measurements are of the total OC contained in the precipitation. This includes not only the particulate OC but also dissolved organic carbon (DOC) from the adsorption of gaseous organic compounds. In fact, the DOC component of the organic carbon is the main component. The situation is fur-

Table 8. Comparison of Modeled and Measured Wet Deposition of BC in ECHAM

Station	Latitude	Longitude	Modelled, μg L^{-1}	Measurement, μg L^{-1}	Time Period
Alert	82°30'N	62°30'W	3 - 4.3	45.5 (0-127)a	Nov.-Dec. 1983
Greenland Sea	79°48'N	4°12'W	20.7	38.7 (5.4-75.5) a	July 1983
Spitzbergen	79°N	12°E	12.2	31 (6.7-52)a	May 1983
Summit	72°N	38°5'W	3.4	5.4 b	annual
Barrow	71°18'N	156°36'W	6.7 - 7.9	23 (7.3-60.4) a	March-April 1983
Abisko	68°18'N	18°30'E	22.5 - 24.4	33 (8.8-77) a	March-April 1984
North Sweden	66°N	20°E	32.1 - 61.8	172 (30-700) c	April-Aug. 1981
South Sweden	60°N	16°E	71.9 - 129.5	193 (20-600) c	April-Aug. 1981
Mace Head	53°18'N	9°54'W	9.6 - 16.6	31 (9-94) d	Oct.-Nov. 1989
Gif sur Yvette	49°N	2°E	95.5	333 (27-1348) d	1988-1990
Porspoder	48°30'N	4°46'W	34.9	31 e	March 1994
Hurricane Hill	48°N	123°30'W	18.7	14.7 (10.1-18.5) a	April 1984
Seattle	47°36'N	122°18'W	13.6 - 18.2	60 (28-130) c	Dec. 1980-Jan. 1981

The range in the modeled values is the range of the monthly modeled means for the same period as the measurements. Here, a, *Clarke and Noone* [1985]; b, *Pertuisot* [1997]; c, *Ogren et al.* [1984]; d, *Ducret and Cachier* [1992].

ther complicated by the dissolution of OC aerosol once it has been introduced into cloud or rain drops. This has the effect of reducing the observed particulate OC content and should lead to an overestimation by the model of the wet deposition of OC aerosol when compared with observations. This reduction of OC in the particulate phase in precipitation may be of the order of 20% [*Ducret and Cachier*, 1992]. A summary of measurements of OC are presented in Table 10. The model generally underestimates the wet deposition of OC by a factor of 2-7. This is a similar underestimation to what we have seen with the aerosol measurements, which suggests the importance of secondary and natural sources for the production of hydrophilic particulate OC. An additional factor near source regions may be washout of particulate OC in precipitation events.

7. Radiative Impact

We now calculate and discuss the direct radiative forcing of carbonaceous aerosol from fossil fuel combustion. We have shown that secondary OC aerosol appears rapidly within a grid cell and may increase the burden by a factor of 2 (section 6.2). We will therefore double the loading of OC in these calculations to attempt to account for secondary OC. An external mixture of the components is assumed when calculating the radiative forcing, an assumption which is not a true representation of reality. However, the spatial and temporal variability of the mixture of the aerosol and the uncertainty in the optical properties of internally mixed aerosol mean that an external mixture of the aerosol is probably the most acceptable assumption we can make. For radiative purposes an external mixture of the aerosol and cloud droplets is also assumed within clouds.

The radiative forcing is calculated at each radiative time step on the basis of the instantaneous concentrations of the aerosol components. Radiative forcing is defined as the difference in the net radiation at the tropopause (190-hPa level) when the aerosol is included in the radiation calculations, as compared to a control experiment without the aerosols. The dynamics of the model are not affected by the inclusion of the aerosols. The optical properties of the "global aerosol data set" (GADS) climatology [*Koepke et al.*, 1997] have been used in this work. We assume that the hydrophilic organic carbon aerosol has the optical properties of the "water soluble" aerosol. Because of the organic nature of the hydrophobic OC aerosol, it is also assumed to be similar to "water soluble" aerosol, but in this case at a relative humidity of 0%. The optical properties of the "soot" aerosol in the work of *Koepke et al.* [1997] are assumed for the BC aerosol. These properties are given in Table 11.

A direct link between the burden of aerosol and the forcing is not possible because of the influence of other parameters such as the underlying albedo. Over areas with low surface albedo the scattering effect of the

Table 9. Comparison of Modeled and Measured Organic Carbon Concentration at Various Sites Around the Globe.

Station	Latitude	Longitude	Concentration, ng $^{-3}$ Modeled	Measured	Time Period
	Island Sites: Model/Measured Ratio = 0.167				
Greenland	70°N	40°W	1.6	158 a	Dec.
North Atlantic	42°30'N	14°W	23	175.5 b,c	Oct.-Nov.
Corsica	42°N	9°E	422	1517 d	spring
Oki Island	36°N	133°E	549	1417 e	annual
St. Nicholas Island	33°9'N	119°18'W	137 - 303	524 - 1400 f	Oct.-Nov.
Hachi-jima	33°5'N	139°45'E	222 - 255	900 - 1300 g	Dec.-Jan.
Bermuda	32°45'N	65°W	12 - 35	570 - 770 h,i	Feb.-March
Chichi-jima	27°N	142°E	130	700 g	Dec.
Mauna Loa	20°N	157°30'W	8	50 j	annual
Pacific	1°36' to 5°30'N	81°W	12	417 h	Feb.
	Rural Sites: Model/Measured Ratio = 0.174				
Barrow	71°10'N	156°20'W	8 - 25	1313 k	Jan.-April
Mace Head	53°18'N	9°54'W	139	1024 l	annual
Gif sur Yvette	48°42'N	2°8'E	774	5750 d	annual
Landes	44°N	1°W	239	1500 d	autumn
Abastumani	41°30'N	42°40'E	1178	2500 m	July
Allegheny	40°N	79°W	522	2150 n	Aug.
Puerto Rico	18°15'N	66°45'W	54	500 o	March
Peru	10°S	76°W	20	160 p	March-April
	Urban Sites: Model/Measured Ratio = 0.333				
Leeds	53°48'N	1°34'W	524 - 778	918 - 1530 q	summer,winter
Berlin	52°30'N	13°20'E	10741	16654 r	winter
Paris	48°50'N	2°20'E	1124	9400 d	annual
Beijing	40°N	116°E	2989	3214 s	April
Nagoya	35°10'N	136°50'E	549	16225 t	annual
Los Angeles	34°4'N	118°15'W	900	7300 u	annual
Guiyang	26°30'N	106°45'E	2593	11071 s	June
Guangzhou	23°N	113°E	2256	5952 s	March
Hong Kong	22°N	114°E	1175	7620 v	Dec.
Ecuador	2°S	77°18'W	90	510 w	annual

The range in the modeled values is the range of the monthly modeled means for the same period as the measurements. Here, a, *Pertuisot* [1997]; b, *Ketsidiris et al.* [1976]; c, *Andreae* [1983]; d, *Cachier et al.* [1989]; e, *Mukai et al.* [1990]; f, *Hidy et al.* [1974]; g, *Ohta and Okita* [1984]; h, *Wolff et al.* [1986]; i, *Hoffman and Duce* [1977]; j, *Clarke* [1989]; k, *Gaffney et al.* [1984]; l, *Cachier et al.* [1994]; m, *Dzubay et al.* [1984]; n, *Keeler et al.* [1990]; o, *Novakov and Penner* [1993]; p, *Cachier et al.* [1986]; q, *Willison et al.* [1985]; r, *Shen and Israel* [1989]; s, *Simoneit et al.* [1991]; t, *Kadowaki* [1990]; u, *Gray et al.* [1984]; v, *Zheng et al.* [1997]; w, *Andreae et al.* [1984].

Table 10. Comparison of Modeled and Measured Wet Deposition of Organic Carbon in ECHAM.

Station	Latitude	Longitude	Particulate Organic Carbon C_o, μg L^{-1} Modeled	Measured	Time Period
Rörvik	57°12'N	12°18'E	182	237 a	Dec.-March
Mace Head	53°18'N	9°54'W	17 - 23	69 b	Oct.-Nov. 1989
Porspoder	48°30'N	4°46'W	52	135 c	March 1994
Gif sur Yvette	48°N	2°E	129	851 b	1988-1990

The range in the modeled values is the range of the monthly modeled means for the same period as the measurements. Here, a, *Brorström-Lundén and Lovblad* [1991]; b, *Ducret and Cachier* [1992]; c, *Pertuisot* [1997].

Table 11. Optical (extinction coefficient σ(e) and Single Scatter Albedo SSA at λ=500nm) and Physical Properties of the Aerosols in the Dry State (0% RH) Used in Calculating the Short Wave Radiative Forcing

Species	σ(e) m^2g^{-1}	SSA	Radius μm	Geo Dev.	Density g cm^{-3}
OC	3.6	0.98	0.0212	2.24	1.8
BC	11	0.23	0.0118	2	1.0

aerosol dominates, leading to a negative forcing. Over areas of high surface albedo, over cloudy areas, and in areas with large concentrations of scattering aerosol, the absorbing aerosol has the opportunity to absorb the reflected or scattered solar radiation, and therefore the forcing of these aerosols is enhanced, resulting in a positive forcing.

Figure 11 shows the distribution of the annual average radiative forcing due to BC and OC aerosol at the top of the troposphere when clouds are included in the general circulation model (GCM) calculations. The forcing due to fossil fuel carbonaceous aerosol is generally confined to land areas of the Northern Hemisphere. Positive forcing may be seen over areas of high albedo, such as the Sahara desert and the Arctic. An interesting feature is the large positive forcing over China. This may be explained by the high areal cloud coverage in the model in this region. Significant amounts of BC aerosol advecting over these clouds will greatly affect the absorption and therefore the forcing of the total aerosol. No significant warming is found in the Southern Hemisphere. This is not surprising as this study concentrates on the radiative effect of fossil fuel emissions, which are predominantly found in the Northern Hemisphere.

In Table 12 we compare the normalized forcings calculated here to those from various authors. The normalized forcings will eliminate the variations due to differences in the column burdens of aerosol. The works of *Haywood et al.* [1997] (hereinafter referred to as H97) and *Myhre et al.* [1999] (hereinafter referred to as M99) prescribe the SO_4 burdens of *Langner and Rodhe* [1991] and *Restad et al.* [1998], respectively, and then assign a constant 7.5% BC fraction before calculating the solar forcing. The work of *Haywood and Ramaswamy* [1998] (hereinafter referred to as H98) used a scaled "best guess" estimate of the *Cooke and Wilson* [1996] BC distribution. The normalized forcings for SO_4 in these works and that of *Feichter et al.* [1997], which used the ECHAM4 model, are within 20% of each other.

The normalized BC forcings of the work presented here, and of H97, HR98, and M99 when clouds are included are within 50% of each other. When clouds are excluded, there is a much larger range. The inclusion of clouds increases the normalized forcing of this work and M98, while it decreases for H97 and HR98. This is probably due to the vertical distribution of the BC aerosol. It would appear that the effect of clouds on the solar forcing is not as great as suggested by these previous works. The differences in the sensitivity of the forcing is due to the fact that in all the other works the authors prescribed the BC distribution according to the SO_4 distribution and therefore there are no interferences between cloud cover and aerosol distribution, but, in fact, aerosol concentration depends very much on the occurrence of clouds and precipitation.

The normalized OC forcing appears to be approximately 50% of that of sulfate if one compares with the sulfate forcing calculated with the same model [*Feichter et al.*, 1997]. One may therefore speculate that the global forcing of OC aerosol would be approximately 50% of that of sulfate if OC is as important an aerosol species as sulfate [*Cachier et al.*, 1990; *Novakov and Corrigan*, 1996; *Hegg et al.*, 1997].

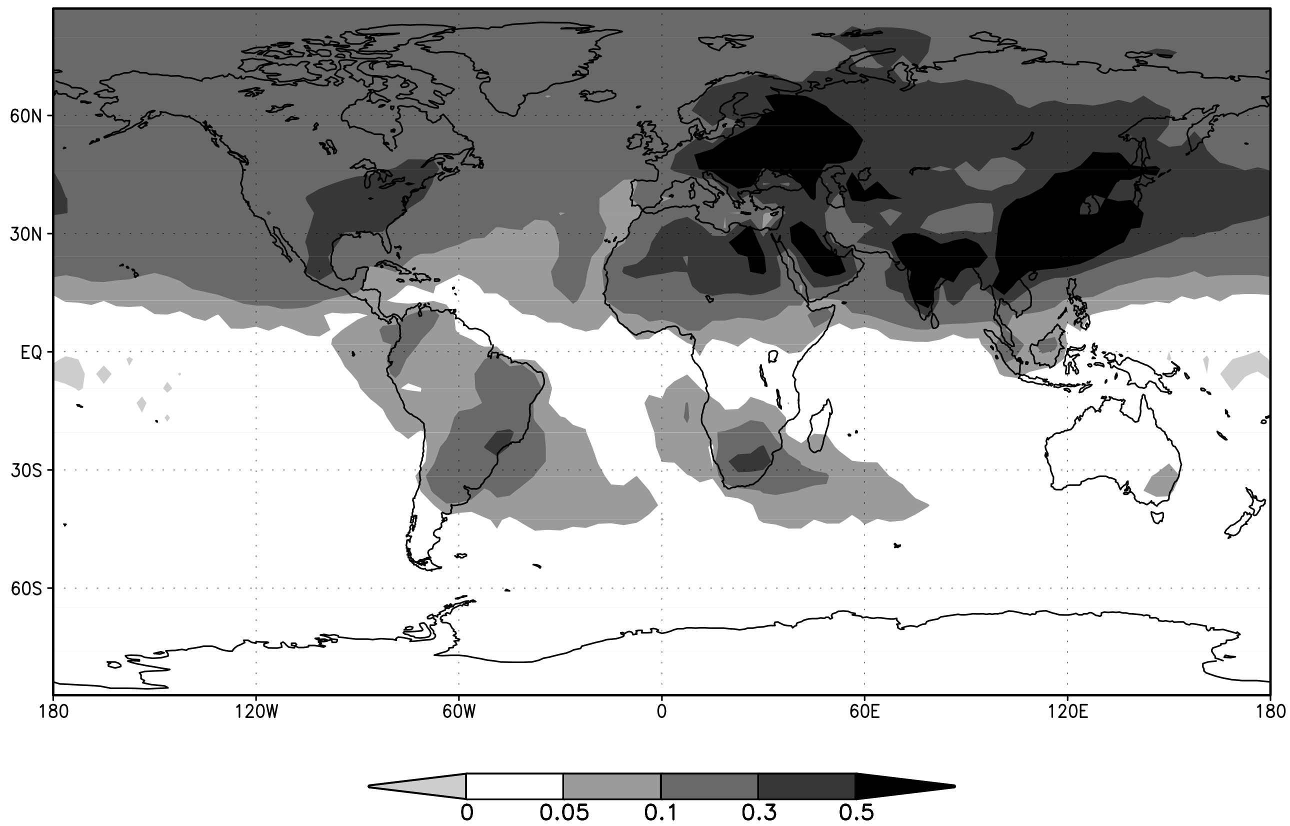

Figure 11. The annual average radiative forcing (W m^{-2}) due to BC and 2×OC from fossil fuel combustion.

Table 12. Comparison of Solar Radiative Forcing (W m^{-2}), Burdens and Normalised Forcings by External Mixtures of Fossil Fuel Derived Sulphate, BC and OC With Other Authors

Author	Species	Burden mg m^{-2}	Radiative forcing W m^{-2}		Normalized forcing W g^{-1}	
			Inc. Clouds	Exc. Clouds	Inc. Clouds	Exc. Clouds
This work	BC	0.143	0.173	0.154	1210	1077
	OC×2	0.341	-0.024	-0.050	-70	-147
H97	BC 7.5%	0.13	0.20	0.28	1538	2153
HR98	BC	0.25*	0.4	0.44	1600	1760
M99	BC 7.5%	0.14	0.16	0.12	1142	857
F97	SO_4	2.23	-0.35		-157	

H97, *Haywood et al.* [1997]; HR98, *Haywood and Ramaswamy* [1998]; M99, *Myhre et al.* [1999]; F97, *Feichter et al.* [1997].
* Includes burden from biomass burning.

8. Conclusions

8.1. Emissions

There is a need to measure the emission factors of carbonaceous aerosol from a wide range of fuels. In addition to this, these emission factors should be measured not only in the industrialized countries but also in less developed regions or at the very least in conditions which are representative of these regions, and BC and OC emission factors should be measured concurrently in order to retrieve some information on the ratio of BC and OC in the total carbonaceous aerosol. Lignite brown coal is probably the fuel which needs to investigated first as there have been few, if any, detailed measurements of the carbonaceous fraction of this fuel, which is widely used in the former Eastern European bloc and the former USSR. This fuel type is a major source of carbonaceous aerosol, if the assumptions made in this work are reasonable.

The differentiation between emission factors according to the level of development of a country appears to be very important. We found a large increase in the total emissions of the south and central Americas by taking into account, for example, the differences due to the age of diesel vehicles. While the emission factors derived here are based on what we believe are valid assumptions, in situ measurements of the emission factors would be very useful in determining the uncertainty in this area. From the data available at this time, there appears to be an uncertainty of at least a factor of 2 in the BC and OC emissions. The future trend in emissions depends strongly on the control of emissions from developing nations. If the emission factors assumed in this work for underdeveloped countries are reasonable and are not reduced by the use of more efficient combustion devices or by emission control devices, then the emission of carbonaceous aerosol will increase dramatically as these countries develop. This will probably be crucial in areas like China and eastern Asia.

As global modelers we are interested in the long-range transport of trace species in the atmosphere. The lifetime of submicron aerosol is sufficiently long that it undergoes long-range transport, and therefore we have calculated this fraction of the total carbonaceous aerosol emissions. While our calculations suggest that the reduction in the global emissions is on the order of 25%, it would be highly desirable to have measurements of the size fractionation of carbonaceous aerosol in order to confirm this. In résumé, we recommend that emission factors for carbonaceous aerosol be measured for a greater number of fuels than at present, in situations representative of their use in different environments of the globe, and measured in such a way as to calculate the aerosol fraction which is liable to transport over great distances.

At present, emission factors are still based on submicron emission factors with various assumptions having to be made in order to infer carbonaceous aerosol emission factors. These assumptions may lead to great uncertainty in the global carbonaceous emission inventory and should be tested rigorously. These assumptions would not be necessary if adequate emission factor measurements were made.

8.2. Model

The model of carbonaceous aerosol used here reproduces the global distribution of BC as measured at surface sites over a large part of the Northern Hemisphere to within the natural variability of the measurements. There appears to be a problem with the transport scheme in the Arctic regions, where haze events are not reproduced successfully. The vertical distribution of BC in the model suggests that the vertical transport of BC may be too strong. Convective events may transport too much hydrophobic BC aerosol above cloud level, where the lifetime of aerosols may be several weeks.

The primary emissions of organic aerosol from fossil fuel use do not represent the total global organic aerosol emission. Therefore the global distribution of OC is not reproduced in a satisfactory manner. The best agreement is found near the source areas, while the least agreement is found in remote areas. It is therefore necessary to implement natural sources of organic aerosol as well as the secondary production of organic aerosol from anthropogenic gaseous precursors. A comparison of the modeled and measured OC concentrations suggests that secondary production of OC aerosol close to primary source regions may account for 50% of the fossil fuel emissions. This assumption underlines the need of understanding the mechanisms of production of particulate anthropogenic secondary organics.

8.3. Radiative

The effect of adding BC and OC in calculating the radiative forcing of fossil fuel aerosol is a reduction by approximately 40% when compared to sulphate on its own. The radiative forcing is quite uncertain, however, because of the uncertainty in the atmospheric burden of aerosol, particularly OC. The fact that the aerosol layer is optically thin means that the forcing of the carbonaceous aerosol can be linearly scaled with the atmospheric burden. Therefore, assuming that the atmospheric burden is linearly related to the emissions, one can say that the forcings are also uncertain to at least a factor of 2. The emissions from fossil fuels do not appear to greatly affect the Southern Hemisphere.

The differences between the radiative forcings calculated in this work and those of other workers show the need to use a consistent and reasonable model of aerosol emission. We believe that the model presented here is an important step this far in calculating the radiative effects of fossil fuel aerosols. Significant improvements will be also gained in the future with a better constraint of organic aerosol fields. The introduction of biomass-burning particles will also enhance the global importance of this type of aerosol.

Finally, we show that because of their significant optical absorption, BC particles could partly offset the cooling effect of sulfates. In this work the warming effect of BC is found to be slightly lower than that presented in previous published papers. Our results point out the need to obtain accurate absorption coefficients for BC particles in external and internal mixtures.

Acknowledgments. This work was supported by the European Commission Environment Project, SINDICATE, ENV4-CT97-0483.

References

Adams, K. M., L. I. Davis Jr., S. M. Japar, D. R. Finley, and R. A. Cary, Measurement of atmospheric elemental carbon: Real-time data for Los Angeles during summer 1987, *Atmos. Environ., Part A*, *24*, 597–604, 1990.

Andreae, M. O., Soot carbon and excess fine potassium : Long-range transport of combustion-derived aerosols, *Science*, *220*, 1148–1151, 1983.

Andreae, M. O., T. W. Andreae, R. J. Ferek, and H. Raemdonck, Long range transport of soot carbon in the marine atmosphere, *Sci.Total Environ.*, *36*, 73–80, 1984.

Ball, D. J., Particulate carbon emissions and diesel vehicles, 1987, paper presented at Institution of Mechanical Engineers Conference on Vehicle Emissions and Their Impact on European Air Quality.

Barbella, R., C. Bertoli, A. Ciajolo, and A. D'Anna, Soot and unburnt liquid hydrocarbon emissions from diesel engines, *Combust. Sci. Technol.*, *59*, 183–198, 1988.

Bengtsson, L., K. Arpe, E. Roeckner, and U. Schulzweida, Climate predictability experiments with a general circulation model, *Clim. Dyn.*, *12*, 261–278, 1996.

Berner, A., S. Sidla, Z. Galambos, C. Kruisz, R. Hitzenberger, H. M. ten Brink, and G. P. A. Kos, Modal character of atmospheric black carbon size distributions, *J. Geophys. Res.*, *101*, 19,559–19,565, 1996.

Blake, D. F., and K. Kato, Latitudinal distribution of black carbon soot in the upper troposphere and lower stratosphere, *J. Geophys. Res.*, *100*, 7195–7202, 1995.

Bocola, W., and M. C. Cirillo, Air pollutant emissions by combustion processes in Italy, *Atmos. Environ.*, *23*, 17–24, 1989.

Bodhaine, B. A., Aerosol absorption measurements at Barrow, Mauna Loa and the South Pole, *J. Geophys. Res.*, *100*, 8967–8975, 1995.

Bond, T. C., R. J. Charlson, and J. Heintzenberg, Quantifying the emission of light-absorbing particles: Measurements tailored to climate studies, *Geophys. Res. Lett.*, *25*, 337–340, 1998.

Boucher, O., and T. L. Anderson, General circulation model assessment of the sensitivity of direct climate forcing by anthropogenic sulfate aerosols to aerosol size and chemistry, *J. Geophys. Res.*, *100*, 26,117–26,134, 1995.

Brémond, M. P., H. Cachier, and P. Buat-Menard, Particulate carbon in the Paris region atmosphere, *Environ. Technol. Lett.*, *10*, 339–346, 1989.

Brorström-Lundén, E., and G. Lovblad, Deposition of soot related hydrocarbons during long-range transport of pollution to Sweden, *Atmos. Environ., Part A*, *25*, 2251–2257, 1991.

Brorström-Lundén, E., A. Lindskog, and J. Mowrer, Concentrations and fluxes of organic compounds in the atmosphere of the Swedish west coast, *Atmos. Environ.*, *28*, 3605–3615, 1994.

Brost, R. A., J. Feichter, and M. Heimann, Three-dimensional simulation of ^{7}Be in a global climate model, *J. Geophys. Res.*, *96*, 22,423–22,445, 1991.

Cachier, H., Carbonaceous combustion particles, in *Atmospheric Particles*, edited by R. M. Harrison and R. E. Van Grieken, pp. 295–348, John Wiley, New York, 1998.

Cachier, H., P. Buat-Ménard, M. Fontugne, and R. Chesselet, Long range transport of continentally derived particulate carbon in the marine atmosphere : Evidence from stable carbon isotope studies, *Tellus*, *38B*, 161–177, 1986.

Cachier, H., M.-P. Brémond, and P. Buat-Ménard, Determination of atmospheric soot carbon with a simple thermal method, *Tellus*, *41B*, 379–390, 1989.

Cachier, H., M.-P. Brémond, and P. Buat-Ménard, Organic and black carbon aerosols over marine regions of the northern hemisphere, in *Proceedings of the International Conference on Atmospheric Chemistry*, edited by L. Newman, W. Wang, and C. S. Kiang, pp. 249–261, Brookhaven Natl. Lab., Upton, N.Y., 1990.

Cachier, H., C. Liousse, A. Cachier, B. Ardouin, G. Polian, V. Kazan, and A. D. A. Hansen, Black carbon aerosols at the remote site of Amsterdam Island, 1994, paper presented at the Fifth International Conference on Carbonaceous Aerosols, U.S. Dep. of Energy, Berkeley, Calif., Aug. 23-26, 1994.

Cachier, H., C. Liousse, P. Buat-Ménard, and A. Gaudichet, Particulate content of savanna fire emissions, *J. Atmos. Chem.*, *22*, 123–148, 1995.

Cachier, H., C. Liousse, M.-H. Pertuisot, A. Gaudichet, F. Echalar, and J.-P. Lacaux, African fire particulate emissions and atmospheric influence, in *Biomass Burning and Global Change*, edited by J. S. Levine, pp. 428–440, MIT Press, Cambridge, Mass., 1996.

Cass, G. R., P. M. Boone, and E. S. Macias, Emissions and air quality relationships for atmospheric carbon particles in Los Angeles, in *Particulate Carbon: Atmospheric Life Cycle*, edited by G. T. Wolff and R. L. Klimisch, Plenum, New York, 1982.

Cess, R. D., et al., Intercomparison and interpretation of climate feedback processes in 19 atmospheric general circulation models, *J. Geophys. Res.*, *95*, 16,601–16,615, 1990.

Charlson, R. J., J. Langner, H. Rodhe, C. B. Leovy, and S. G. Warren, Perturbation of the northern hemisphere radiative balance by backscattering from anthropogenic aerosols, *Tellus*, *43AB*, 152–163, 1991.

Charlson, R. J., S. E. Schwartz, J. M. Hales, R. D. Cess, J. A. Coakley Jr., J. E. Hansen, and D. J. Hofmann, Climate forcing by anthropogenic aerosols, *Science*, *255*, 423–430, 1992.

Chýlek, P., et al., Black carbon: Atmospheric concentrations and cloud water content measurements over southern Nova Scotia, *J. Geophys. Res.*, *101*, 29,105–29,110, 1996.

Clarke, A. D., Aerosol light absorption by soot in remote environments, *Aerosol Sci. Technol.*, *10*, 161–171, 1989.

Clarke, A. D., and K. J. Noone, Soot in the Arctic snowpack : A cause for perturbations in radiative transfer, *Atmos. Environ.*, *19*, 2045–2053, 1985.

Clarke, A. D., R. E. Weiss, and R. J. Charlson, Elemental carbon aerosols in the urban, rural, and remote-marine troposphere and in the stratosphere : Inferences from light absorption data and consequences regarding radiative transfer, *Sci. Total Environ.*, *36*, 97–102, 1984.

Cooke, W. F., and J. J. N. Wilson, A global black carbon aerosol model, *J. Geophys. Res.*, *101*, 19,395–19,409, 1996.

Cooke, W. F., S. G. Jennings, and T. G. Spain, Black carbon measurements at Mace Head, 1989-1996, *J. Geophys. Res.*, *102*, 25,339–25,346, 1997.

Countess, R. J., S. H. Cadle, P. J. Groblicki, and G. T. Wolff, Chemical analysis of size-segregated samples of Denver's ambient particulate, *J. Air Pollut. Control Assoc.*, *31*, 247–252, 1981.

Del Delumyea, R., and A. Kalivretenos, Elemental carbon and lead content of fine particles from American and French cities of comparable size and industry, 1985, *Atmos. Environ.*, *21*, 1643–1647, 1987.

Duce, R. A., Speculations on the budget of particulate and vapor phase non-methane organic carbon in the global troposphere, *Pure Appl. Geophys.*, *116*, 244–273, 1978.

Ducret, J., and H. Cachier, Particulate carbon content in rain at various temperate and tropical locations, *J. Atmos. Chem.*, *15*, 55–67, 1992.

Dzubay, T. G., R. K. Stevens, and P. L. Haagenson, Composition and origins of aerosol at a forested mountain in Soviet Georgia, *Environ. Sci. Technol.*, *18*, 873–883, 1984.

Environmental Protection Agency (EPA), National air pollutant emission trends 1900-1994, *Tech. rep.*, Off. of Air Qual. Plann. and Stand., Research Triangle Park, NC, 1994.

EPA, Supplement B to compilation of air pollutant emission factors Volume I: Stationary point and area sources, *Tech. rep.*, Off. of Air Qual. Plann. and Stand., Research Triangle Park, NC, 1996.

Etemad, B., and J. Luciani, *World Energy Production 1800-1985*, p. 272, Librarie DROZ, Geneva, 1991.

Feichter, J., R. A. Brost, and M. Heimann, Three-dimensional modeling of the concentration and deposition of ^{210}Pb aerosols, *J. Geophys. Res.*, *96*, 22,447–22,460, 1991.

Feichter, J., U. Lohmann, and I. Schult, The atmospheric sulfur cycle in ECHAM-4 and its impact on the shortwave radiation, *Clim. Dyn.*, *13*, 235–246, 1997.

Fouquart, Y., and B. Bonnel, Computations of solar heating of the Earth's atmosphere: A new parameterization, *Beitr. Phys. Atmos.*, *53*, 35–62, 1980.

Gaffney, J. S., R. L. Tanner, and M. Phillips, Separating carbonaceous aerosol source terms using thermal evolution, carbon isotopic measurements, and C/N/S determinations, *Sci. Total Environ.*, *36*, 53–60, 1984.

Ganzeveld, L., J. Lelieveld, and G.-J. Roelofs, A dry deposition parametrization for sulfur oxides in a chemistry and general circulation model, *J. Geophys. Res.*, *103*, 5679–5694, 1998.

Gray, H. A., G. R. Cass, J. J. Huntzicker, E. K. Heyerdahl, and J. A. Rau, Elemental and organic carbon particle concentrations : A longterm perspective, *Sci. Total Environ.*, *36*, 17–25, 1984.

Guillemin, M., et al., International round robin test on the measurement of carbon in diesel exhaust particulates, *Int. Arch. Occup. Environ. Health*, *70*, 161–172, 1997.

Hansen, A. D. A., and T. Novakov, Aerosol black carbon measurements over the western Atlantic Ocean, *Global Biogeochem. Cycles*, *2*, 41–45, 1988.

Hansen, A. D. A., and H. Rosen, Individual measurements of the emission factor of aerosol black carbon in automobile plumes, *J. Air Waste Manage. Assoc.*, *40*, 1654–1657, 1990.

Hansen, A. D. A., T. J. Conway, L. P. Steele, B. A. Bodhaine, K. W. Thoning, P. Tans, and T. Novakov, Correlations among combustion effluent species at Barrow, Alaska: Aerosol black carbon, carbon dioxide and methane, *J. Atmos. Chem.*, *9*, 283–299, 1989.

Hansen, A. D. A., V. N. Kapustin, V. M. Kopeikin, D. A. Gillette, and B. A. Bodhaine, Optical absorption by aerosol black carbon and dust in a desert region of central Asia, *Atmos. Environ., Part A*, *27*, 2527–2531, 1993.

Haywood, J. M., and V. Ramaswamy, Global sensitivity studies of the direct radiative forcing due to anthropogenic sulfate and black carbon aerosols, *J. Geophys. Res.*, *103*, 6043–6058, 1998.

Haywood, J. M., and K. P. Shine, The effect of anthropogenic sulfate and soot aerosol on the clear sky planetary radiation budget, *Geophys. Res. Lett.*, *22*, 603–605, 1995.

Haywood, J. M., D. L. Roberts, A. Slingo, J. M. Edwards, and K. P. Shine, General circulation model calculations of the direct radiative forcing by anthropogenic sulfate and fossil-fuel soot aerosol, *J. Clim.*, *10*, 1562–1577, 1997.

Hegg, D. A., J. Livingston, P. V. Hobbs, T. Novakov, and P. Russell, Chemical apportionment of aerosol column optical depth off the mid-Atlantic coast of the United States, *J. Geophys. Res.*, *102*, 25,293–25,303, 1997.

Heintzenberg, J., Size-segregated measurements of particulate elemental carbon and aerosol light absorption at remote Arctic locations, *Atmos. Environ.*, *16*, 2461–2469, 1982.

Heintzenberg, J., and A. Mészáros, Elemental carbon, sulfur and metals in aerosol samples at a Hungarian regional air pollution station, *Idöjáràs*, *89*, 313–319, 1985.

Heintzenberg, J., R. J. Charlson, A. D. Clarke, C. Liousse, V. Ramaswamy, K. P. Shine, M. Wendisch, and G. Helas, Measurements and modelling of aerosol single-scattering albedo: Progress, problems and prospects, *Beitr. Phys. Atmos.*, *70*, 249–263, 1997.

Hidy, G. M., P. K. Mueller, H. H. Wang, J. Karney, S. Twiss, M. Imada, and A. Alcocer, Observations of aerosols over southern California coastal waters, *J. Appl. Meteorol.*, *13*, 96–107, 1974.

Hobbs, P. V., J. S. Reid, R. A. Kotchenruther, R. J. Ferek, and R. Weiss, Direct radiative forcing by smoke from biomass burning, *Science*, *275*, 1776–1778, 1997.

Hoffman, E. J., and R. A. Duce, Organic carbon in marine atmospheric particulate matter: Concentration and particle size distribution, *Geophys. Res. Lett.*, *4*, 449–452, 1977.

Horvath, H., I. Kreiner, C. Norek, O. Preining, and B. Georgi, Diesel emissions in Vienna, *Atmos. Environ.*, *22*, 1255–1269, 1988.

Janssen, N. A. H., D. F. M. Van Mansom, K. Van der Jagt, H. Harssema, and G. Hoek, Mass concentration and elemental composition of airborne particulate matter at street and background locations, *Atmos. Environ.*, *31*, 1185–1193, 1997.

Kadowaki, S., Characterization of carbonaceous aerosols in the Nagoya urban area, 1, Elemental and organic carbon concentrations and the origin of organic aerosols, *Environ. Sci. Technol.*, *24*, 741–744, 1990.

Keeler, G. J., S. M. Japar, W. W. Brachaczek, R. A. Gorse, J. M. Norbeck, and W. R. Pierson, The sources of aerosol elemental carbon at Allegheny Mountain, *Atmos. Environ., Part A*, *24*, 2795–2805, 1990.

Ketsidiris, G., J. Hahn, R. Jaenicke, and C. Junge, The organic constituents of atmospheric particulate matter, *Atmos. Environ.*, *10*, 603–610, 1976.

Kiehl, J. T., and B. P. Briegleb, The relative roles of sulfate aerosols and greenhouse gases in climate forcing, *Science*, *260*, 311–314, 1993.

Koepke, P., M. Hess, I. Schult, and E. P. Shettle, Global aerosol data set, *Tech. Rep. 243*, Max Planck Inst., Hamburg, Germany, 1997.

Kopeykin, V. M., V. N. Kapustin, and M. S. Pekur, Monitoring of soot aerosol in the atmosphere of Moscow, *Izv. Acad. Sci. USSR Atmos. Oceanic Phys. Engl. Transl.*, *29*, 198–202, 1993.

Langner, J., and H. Rodhe, A global three-dimensional model of the tropospheric sulfur cycle, *J. Atm. Chem.*, *13*, 225–263, 1991.

Larson, S. M., G. R. Cass, and H. A. Gray, Atmospheric carbon particles and the Los Angeles visibilty problem, *Aerosol Sci. Technol.*, *10*, 118–130, 1989.

Latif, M., J. Biercamp, H. v. Storch, M. J. McPhaden, and E. Kirk, Simulation of ENSO related surface wind anomalies with an atmospheric GCM forced by observed SST, *J. Clim.*, *3*, 509–521, 1990.

Legrand, M., M. De Angelis, T. Staffelbach, A. Neftel, and B. Stauffer, Large perturbations of ammonium and organic acids content in the Summit-Greenland ice core, Fingerprint from forest fires?, *Geophys. Res. Lett.*, *19*, 473–475, 1992.

Liousse, C., H. Cachier, and S. G. Jennings, Optical and thermal measurements of black carbon aerosol content in different environments: Variation of the specific attenuation cross section, σ, *Atmos. Environ., Part A*, *27*, 1203–1211, 1993.

Liousse, C., J. E. Penner, C. Chuang, J. J. Walton, H. Eddleman, and H. Cachier, A global three-dimensional model study of carbonaceous aerosols, *J. Geophys. Res.*, *101*, 19,411–19,432, 1996.

Lohmann, U., and E. Roeckner, Influence of cirrus cloud radiative forcing on climate and climate sensitivity in a general circulation model, *J. Geophys. Res.*, *100*, 16,305–16,323, 1995.

Lohmann, U., E. Roeckner, W. D. Collins, A. J. Heymsfield, G. M. McFarquhar, and T. P. Barnett, The role of water vapor and convection during the Central Equatorial Pacific Experiment from observations and model simulations, *J. Geophys. Res.*, *100*, 26,229–26,245, 1995.

Lowenthal, D. H., B. Zielinska, J. C. Chow, J. G. Watson, M. Gautam, D. H. Ferguson, G. R. Neuroth, and K. D. Stevens, Characterization of heavy-duty diesel vehicle emissions, *Atmos. Environ.*, *28*, 731–743, 1994.

Lyubovtseva, Y. S., and L. G. Yatskovich, Soot in the aerosols of different regions, *J. Aerosol Sci.*, *20*, 1269–1272, 1989.

McElroy, M. W., R. C. Carr, D. S. Ensor, and G. R. Markowski, Size distribution of fine particles from coal combustion, *Science*, *215*, 13–19, 1982.

Morcrette, J.-J., Radiation and cloud radiative properties in the European Centre Medium-Range Weather Forecasts forecasting system, *J. Geophys. Res.*, *96*, 9121–9132, 1991.

Muhlbaier, J. L., and R. L. Williams, Fireplaces, furnaces and vehicles as emission sources of particulate carbon, in *Particulate Carbon: Atmospheric Life Cycle*, edited by G. T. Wolff and R. L. Klimisch, pp. 185–205, Plenum, New York, 1982.

Mukai, H., Y. Ambe, K. Shibata, T. Muku, K. Takeshita, T.Fukuma, J. Takahashi, and S. Mizota, Long term variation of chemical composition of atmospheric aerosol on the Oki Islands in the Sea of Japan, *Atmos. Environ., Part A*, *24*, 1379–1390, 1990.

Myhre, G., F. Stordal, K. Restad, and I. S. A. Isaksen, Estimates of the direct radiative forcing due to sulfate and soot aerosols, *Tellus*, *50B*, 463–377, 1999.

Noone, K. J., and A. D. Clarke, Soot scavenging measurements in Arctic snowfall, *Atmos. Environ.*, *22*, 2773–2778, 1988.

Novakov, T., and C. E. Corrigan, Cloud condensation nucleus activity of the organic component of biomass smoke particles, *Geophys. Res. Lett.*, *23*, 2141–2144, 1996.

Novakov, T., and J. E. Penner, Large contributions of organic aerosols to cloud-condensation-nuclei concentrations, *Nature*, *365*, 823–826, 1993.

O'Dowd, C. D., M. H. Smith, and S. G. Jennings, Submicron particle, radon, and soot carbon characteristics over the northeast Atlantic, *J. Geophys. Res.*, *98*, 1123–1135, 1993.

Ogren, J. A., P. J. Groblicki, and R. J. Charlson, Measurement of the removal rate of elemental carbon from the atmosphere, *Sci. Total Environ.*, *36*, 329–338, 1984.

Ohta, S., and T. Okita, Measurements of particulate carbon in urban and marine air in Japanese areas, *Atmos. Environ.*, *18*, 2439–2445, 1984.

Parungo, F., C. Nagamoto, M.-Y. Zhou, A. D. A. Hansen, and J. Harris, Aeolian transport of aerosol black carbon from China to the ocean, *Atmos. Environ.*, *28*, 3251–3260, 1994.

Penner, J. E., S. J. Ghan, and J. J. Walton, The role of biomass burning in the budget and cycle of carbonaceous soot aerosols and their climate impact.

Penner, J. E., R. E. Dickinson, and C. A. O'Neill, Effects of aerosol from biomass burning on the global radiation budget, *Science*, *256*, 1432–1433, 1992.

Penner, J. E., H. Eddleman, and T. Novakov, Towards the development of a global inventory for black carbon emissions, *Atmos. Environ., Part A*, *27*, 1277–1295, 1993.

Penner, J. E., R. C. Easter, and S. J. Ghan, A parameterization of cloud droplet nucleation, II Multiple aerosol types, *Atmos. Res.*, *36*, 39, 1995.

Pertuisot, M. H., Transfert du carbone atmosphérique dans les neiges et les pluies, Ph.D. thesis, Univ. Paris 7, Paris, 1997.

Polissar, A. V., Measurements of the soot mass concentration and particle-size distribution of atmospheric aerosol in the eastern Arctic, *Izv. Acad. Sci. USSR Atmos. Oceanic Phys. Engl. Transl.*, *29*, 66–73, 1993.

Pueschel, R. F., D. F. Blake, K. G. Snetsinger, A. D. A. Hansen, S. Verma, and K. Kato, Black carbon (soot) aerosol in the lower stratosphere and upper troposphere, *Geophys. Res. Lett.*, *19*, 1659–1662, 1992.

Raunemaa, T., K. Kuuspalo, T. Alander, E. Tamm, A. Mirme, and V. Laine, Black carbon and aerosol in Böisto Island, *J. Aerosol Sci.*, *24*, S29–S30, 1993.

Restad, K., I. S. A. Isaksen, and T. K. Berntsen, Global distribution of sulphate in the troposphere. a three-dimensional model study, *Atmos. Environ.*, *32*, 3593–3609, 1998.

Roeckner, E., Parameterization of cloud radiative properties in the ECHAM4 model, 1995, paper presented at WCRP workshop on Cloud microphysics parameterizations in global atmospheric circulation models, World Climate Research Program, Kananaskis, Canada, 23-25 May, 1995.

Roeckner, E., et al., Simulation of the present-day climate with the ECHAM model: Impact of model physics and resolution, *Tech. rep.*, Max-Planck-Inst. für Meteorol., Hamburg, Germany, 1992.

Roeckner, E., et al., The atmospheric general circulation model ECHAM-4: Model description and simulation of present-day climate, *Tech. Rep. 218*, Max-Planck-Institute für Meteorologie, Hamburg, Germany, 1996.

Rogge, W. F., M. A. Mazurek, L. M. Hildemann, G. R. Cass, and B. R. T. Simoneit, Quantification of urban organic aerosols at amolecular level: Identification, abundance and seasonal variation, *Atmos. Environ., Part A*, *27*, 1309–1330, 1993.

Rosen, H., and A. D. A. Hansen, Role of combustion-generated carbon particles in the absorption of solar radiation in the Arctic haze, *Geophys. Res. Lett.*, *11*, 461–464, 1984.

Rosen, H., and A. D. A. Hansen, Estimates of springtime soot and sulfur fluxes entering the Arctic troposphere: Implications to source regions, *Atmos. Environ.*, *19*, 2203–2207, 1985.

Rotty, R. M., Estimates of seasonal variation in fossil fuel CO_2 emissions, *Tellus*, *39*, 184–202, 1987.

Schult, I., J. Feichter, and W. F. Cooke, The effect of black carbon and sulfate aerosols on the global radiation budget, *J. Geophys. Res.*, *102*, 30,107–30,117, 1997.

Schure, M. R., P. A. Soltys, D. F. S. Natusch, and T. Mauney, Surface area and porosity of coal fly ash, *Environ. Sci. Technol.*, *19*, 82–86, 1985.

Shen, J., and G. W. Israel, A receptor model using a specific non-negative transformation technique for ambient aerosol, *Atmos. Environ.*, *23*, 2289–2298, 1989.

Simoneit, B. R. T., G. Sheng, X. Chen, J. Fu, J. Zhang, and Y. Xu, Molecular marker study of extractable organic matter in aerosols from urban areas of China, *Atmos. Environ., Part A*, *25*, 2111–2129, 1991.

Smith, D. M., M. S. Akhter, J. A. Jassim, C. A. Sergides, W. F. Welch, and A. R. Chughtai, Studies of the structure and reactivity of soot, *Aerosol Sci. Technol.*, *10*, 311–325, 1989.

Sundqvist, H., A parameterization scheme for non-convective condensation including prediction of cloud water content, *Q. J. R. Meteorol. Soc.*, *104*, 677–690, 1978.

Taylor, K. E., and J. E. Penner, Response of the climate system to atmospheric aerosols and greenhouse gases, *Nature*, *369*, 734–737, 1994.

Tegen, I., and A. A. Lacis, Modeling of particle size distribution and its influence on the radiative properties of mineral dust aerosol, *J. Geophys. Res.*, *101*, 19,237–19,244, 1996.

Tegen, I., A. A. Lacis, and I. Fung, The influence of mineral aerosol from disturbed soils on the global radiation budget, *Nature*, *330*, 419–422, 1996.

Turco, R. P., Global cycle of particulate elemental carbon: a theoretical assessment, in *Proceedings of the Fourth International Conference on Precipitation Scavenging, Dry Deposition, and Resuspension, vol. 2, Dry Deposition and Resuspension*, pp. 1337–1351, Elsevier Sci., New York, 1983.

United Nations, The United Nations energy statistics database (1991), *Tech. rep.*, Stat. Div., New York, 1993.

Weingartner, E., C. Keller, W. A. Stahel, H. Burtscher, and U. Baltensperger, Aerosol emissions in a road tunnel, *Atmos. Environ.*, *31*, 451–462, 1997.

Whitby, K. T., Size distribution and physical properties of combustion aerosols, 1978, paper presented at 1st Conference on Carbonaceous Aerosols, Lawrence Berkeley Lab., Berkeley, CA.

Wild, M., A. Ohmura, H. Gilgen, and E. Roeckner, Validation of GCM-simulated radiative fluxes using surface observations, *J. Clim.*, *8*, 1309–1324, 1996.

Williams, D. J., J. W. Milne, S. M. Quigley, D. B. Roberts, and M. C. Kimberlee, Particulate emissions from "in-use" motor vehicles, II, Diesel vehicles, *Atmos. Environ.*, *23*, 2647–2661, 1989a.

Williams, D. J., J. W. Milne, D. B. Roberts, and M. C. Kimberlee, Particulate emissions from "in-use" motor vehicles, I, Spark ignition vehicles, *Atmos. Environ.*, *23*, 2639–2645, 1989b.

Williamson, D. L., and P. J. Rasch, Two-dimensional semi-Lagrangian transport with shape-preserving interpolation, *Mon. Weather Rev.*, *117*, 102–129, 1989.

Willison, M. J., A. G. Clarke, and E. M. Zeki, Seasonal variation in atmospheric aerosol concentration and composition at urban and rural sites in northern England, *Atmos. Environ.*, *19*, 1081–1089, 1985.

Wolff, G. T., M. S. Ruthkosky, D. P. Stroup, P. E. Korsog, M. A. Ferman, G. J. Wendel, and D. H. Stedman, Measurements of SO_x, NO_x and aerosol species on Bermuda, *Atmos. Environ.*, *20*, 1229–1239, 1986.

Yaaqub, R. R., T. D. Davies, T. D. Jickells, and J. M. Miller, Trace elements in daily collected aerosols at a site in southeast England, *Atmos. Environ., Part A*, *25*, 985–996, 1991.

Zhang, X., B. J. Turpin, P. H. McMurry, S. V. Hering, and M. R. Stolzenburg, Mie theory evaluation of species contributions to 1990 wintertime visibility reduction in the Grand Canyon, *J. Air Waste Manage. Assoc.*, *44*, 153–162, 1994.

Zheng, M., T. S. M. Wan, M. Fang, and F. Wang, Characterization of the non-volatile organic compounds in the aerosols of Hong Kong - Identification, abundance and origin, *Atmos. Environ.*, *31*, 227–237, 1997.

Zier, M., Mass concentrations of total dust and soot in the near surface air in east Germany, *J. Aerosol Sci.*, *22*, S597–S600, 1991.

H. Cachier and C. Liousse, Laboratoire des Sciences du Climat et de l'Environnement, Laboratoire Mixte CNRS-CEA, Avenue de la Terrasse, Gif sur Yvette, F-91198, France

W. F. Cooke, Geophysical Fluid Dynamics Laboratory, P.O. Box 308, Forrestal Campus, Princeton, NJ 08542-0308. (wfc@gfdl.gov)

J. Feichter, Max Planck Institut für Meteorologie, Bundesstrasse 55, D-20146, Hamburg, Germany

Received October 2, 1998; revised January 20, 1999; accepted March 3, 1999.